UAV-spray application in vineyards: Flight modes and spray system adjustment effects on canopy deposit, coverage, and off-target losses

(Article begins on next page)

UAV-spray application in vineyards: Flight modes and spray system adjustment effects on canopy deposit, coverage, and off-target losses

A. Biglia [a], M. Grella [a,*], N. Bloise [b], L. Comba [a,c], E. Mozzanini [a], A. Sopegno [a], M. Pittarello [a], E. Dicembrini [a], L. Eloi Alcatrão [a], G. Guglieri [b], P. Balsari [a], D. Ricauda Aimonino [a,1], P. Gay [a]

[a] *Department of Agricultural, Forest and Food Sciences (DiSAFA), Università degli Studi di Torino, Largo Paolo Braccini 2, 10095 Grugliasco, TO, Italy*
[b] *Department of Mechanical and Aerospace Engineering (DIMEAS), Politecnico di Torino, Corso Duca degli Abruzzi 24, 10129 Torino, Italy*
[c] *CNR-IEIIT – Politecnico di Torino, Corso Duca degli Abruzzi 24, 10129 Torino, Italy*

HIGHLIGHTS

- The UAV-spray system flight path plays a key role in vineyards spray applications.
- Conventional nozzle combined with high UAV speed results in higher canopy deposit.
- Spray applications above the canopy maximised deposition compared to broadcast ones.
- Spray applications above the canopy also minimised ground losses.
- Spray volume rate from UAV must be increased to guarantee a minimum deposit density.

GRAPHICAL ABSTRACT
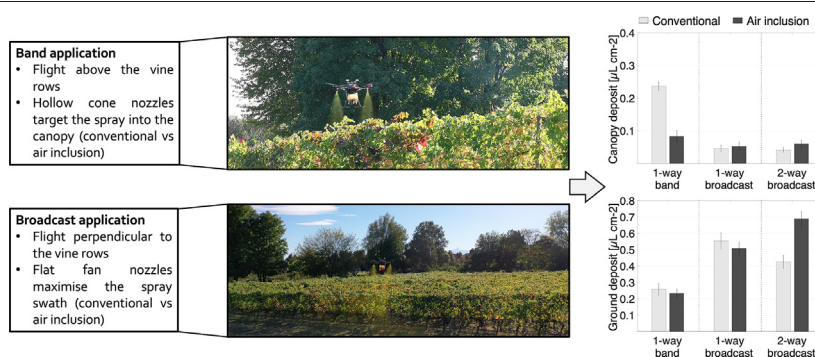
ARTICLE INFO

ABSTRACT

Improvements in the spray application of plant protection products enhance agricultural sustainability by reducing environmental contamination, but by increasing food quality and human safety. Currently, Unmanned Aerial Vehicles (UAVs) are raising interest in spray applications in 3D crops. However, operational configurations of UAV-spray systems need further investigation to maximise the deposition in the canopy and minimise the off-target losses.

Our experimental research focused on investigating the effects on the canopy spray deposition and coverage due to different UAV-spray system configurations. Twelve configurations were tested under field conditions in an experimental vineyard (cv. Barbera), derived from the combination of different UAV flight modes (band and broadcast spray applications), nozzle types (conventional and air inclusion), and UAV cruise speeds (1 and 3 m s^{-1}). Also, the best treatment, among those tested, by using the UAV-spray system and a traditional airblast sprayer were compared. The data was analysed by testing the effects of the three operational parameters and their two- and three-way interactions by means of linear mixed models. The results indicated that the flight mode deeply affects spray application efficiency. Compared to the broadcast spray modes, the band spray mode was able to increase the average canopy deposition from 0.052 to 0.161 μL cm^{-2} (+ 309 %) and reduce the average ground losses from 0.544 to 0.246 μL cm^{-2} (− 54 %). The conventional airblast sprayer, operated at a low spray application rate, showed higher canopy coverage and lower ground losses in comparison to the best UAV-spray system configuration.

* Corresponding author.
  E-mail address: marco.grella@unito.it (M. Grella).
[1] Co-last author.

1. Introduction

In mechanized commercial vineyards, the high number of spray applications during the growing season (Marucco et al., 2019) determines every year an intensive Plant Protection Products (PPPs) use that can cause undesirable effects related to pesticide residues on grapes. The latest European Union report on pesticide residues in food reports exceedance for wine grapes rose from 0.4 to 0.9 % (EFSA, 2021).

Furthermore, during spray applications on bush and/or tree crops with airblast sprayers, only a fraction of the total applied PPP is deposited on the intended target, especially when the sprayers are not adjusted to match it (Grella et al., 2022a). Therefore, a relevant amount of the spray mixture can represent undesirable off-target losses. Such losses are mainly represented by the spray fraction, composed of droplets and/or aerosols and/or vapours depending on chemical PPP properties, that can be transported outside the sprayed area by air currents as spray drift (Grella et al., 2017; Kasner et al., 2021) and by the spray fraction deposited on the ground either directly in the path of the sprayer tractor or beneath the tree rows (Grella et al., 2020a).

Plant protection product applications have changed substantially in recent years with the help of the new European legal framework, beginning with the European Directive for the Sustainable Use of Pesticides 2009/128/EC (EC, 2009), and more recently with the Farm to Fork Strategy for a fair, healthy and environmentally friendly food system, under the aegis of the European Green Deal, which strives to reduce by 50 % the overall use of agrochemicals by 2030 (EC, 2019).

Modern agriculture demands proper pest management to ensure high-quality production (Popp et al., 2013), and thus PPP usage and management have a crucial role in agriculture economic sustainability. In general, the objective of pesticide applications is to precisely, uniformly, and exclusively deliver to the target the minimum amount of active ingredient to achieve the desired biological effect.

In recent years, thanks to the progress of technologies such as the Global Navigation Satellite Systems (GNSS) (Mammarella et al., 2020; Perez-Ruiz et al., 2021) and of hardware able to acquire and process in real-time large amounts of data (Kamilaris et al., 2017; Raikwar et al., 2018; Mammarella et al., 2021a and 2021b) or to read and navigate prescription maps (O'Shaughnessy et al., 2015; Huang et al., 2018; Campos et al., 2019; Hunter et al., 2020), precision agriculture techniques have improved the accuracy of spray applications, especially those related to variable rate applications (Lian et al., 2019; Fabiani et al., 2020; Kayad et al., 2021). This led to proven benefits in reducing environmental and human contamination risks, improving PPP benefits, and raising food quality and safety standards (Rani et al., 2021; Salcedo et al., 2021; Sabzevari and Hofman, 2022). Concurrently, research is also focusing on developing innovative alternative techniques to traditional airblast or pneumatic sprayers, which are generally used in bush or tree crops. These innovative techniques are mainly represented by the Solid Set Canopy Delivery Systems (SSCDS) (Sinha et al., 2020; Imperatore et al., 2021) and spray applications from Unmanned Aerial Vehicles (UAVs) (Xue et al., 2016; Radoglou-Grammatikis et al., 2020; Sassu et al., 2021; Xu et al., 2021). Such techniques are showing promising results for spray applications, especially in complex scenarios where the mechanisation of spray applications represents a challenge to farmers. Among those, aerial spraying from UAVs is challenging in terms of UAV path planning definition (precise and accurate), operational parameters (e.g. spray systems, type of nozzles, etc.), and variable rate spray application. However, aerial spraying from UAVs has been recently spreading worldwide (Chen et al., 2021), particularly in China and many EU countries.

The use of UAVs for spray application purposes is largely used in Asia in arable field crops where it was proven to be a successful technique. Indeed, several in-field experiments on arable crops were carried out in various Asian regions in order to investigate the UAV operational parameters that can affect spray applications the most. In particular, the effects of UAV flight height and cruise speed, and thus the rotors downwash, on canopy spray distribution was investigated mainly in wheat, cotton and rice fields (Lou et al., 2018, Qin et al., 2018; Abd Kharim et al., 2019) by using different types of UAVs, namely helicopters or multirotors (Wang et al., 2017; He et al., 2017; Herbst et al., 2020). Also, the effects of spraying volume and nozzle size on canopy spray deposition were investigated in the field by several authors (Wang et al., 2019a; Ahmad et al., 2020). Furthermore, Wang et al. (2019b) reported some results about the influence of UAV flight modes on wheat canopy spray deposition. The reliability of spray applications from UAVs in arable crops was supported by studies reporting the effective biological efficacy of such aerial treatments (Qin et al., 2016; Lou et al., 2018; Meng et al., 2018; Qin et al., 2018; Wang et al., 2019a).

More recently, interest in using UAVs for spray applications in bush or tree crops has also been rising in Asia, Europe and America with some experiments performed on sugar canes (Zhang et al., 2020), almonds (Li et al., 2021), peaches (Meng et al., 2020), citrus (Zhang et al., 2016; Tang et al., 2018; Martinez-Guanter et al., 2020), olives (Aru et al., 2019; Martinez-Guanter et al., 2020), apples (Li et al., 2018; Liu et al., 2020), pineapples (Wang et al., 2018), arecas (Wang et al., 2020), and vineyards (Giles and Billing, 2015; Sarri et al., 2019; Wang et al., 2021). Generally, the authors mainly investigated operating parameters such as i) cruise speed, ii) flight height, iii) the number of spray passages per each row, iv) nozzle size and type, v) liquid pressure and vi) the number of active nozzles, to better understand their effects on both canopy deposition and coverage. Even if the authors did not agree about the optimal operation parameter settings, all agreed about the consistent effects due to the combination of UAV flight height and cruise speed (OECD, 2021); also, for their case study, the authors evaluated the economic and/or technical feasibility of spray applications when using UAVs compared to conventional spray application techniques. Indeed, the effects of the UAV rotors downwash, which increases the canopy deposition in arable crops (Guo et al., 2019), is extremely important in bush or tree crops where it is used to move foliage and convey the droplets into the canopy, thus increasing the chances to reach the innermost leaves (Zhan et al., 2022). In this respect, Tang et al. (2018), working in citrus orchards, underlined the difficulties in penetrating the canopies according to their shape and density. A relevant aspect raised by the researchers, which is specific to UAV-spray applications, is related to the UAV path and flight mode with respect to the planting system and tree shapes. For example, Giles and Billing (2015) found differences for canopy spray deposition in espalier trellised vineyards by flying across or along the vine rows, while Meng et al. (2020) obtained optimal canopy deposition by varying the flight path according to the peach tree shapes. Since an adequate and homogeneous spray deposition throughout the canopy volume represents, to date, the best strategy to contain both pests and diseases, in each type of crop, the UAV spraying performance needs detailed evaluations and the effects of the UAV operational parameters have to be characterised and therefore properly optimised.

In this context, the main objective of our experimental work was to evaluate the performance of a UAV-spray system in a vertical shoot trellised vineyards at full growth stage, when the canopy density is at its maximum. The performance of the UAV-spray system was compared to that of a conventional ground-based spray application machine, which is an axial fan sprayer coupled with a tractor. Three different flight modes were evaluated for their effect on both canopy deposition and coverage, as well as ground losses. Concurrently, two cruise speeds (1 and 3 m s^{-1}), combined with different nozzle types (conventional and air inclusion), were investigated.

2. Materials and methods

2.1. UAV-spray system

The UAV used for trials spray applications was a hexacopter DJI Matrice 600 Pro (DJI, China), equipped with a customised standalone sprayer system (Fig. 1a) and a D-RTK (Real-Time Kinematic) GNSS (Global Navigation Satellite System) receiver, connected to a ground station. The rotors downwash characterisation for the UAV used in this experimental research is reported in Bloise et al. (2021). Briefly, the region beneath the rotors is characterised by an axial velocity that varies from 8 to 15 m s^{-1}
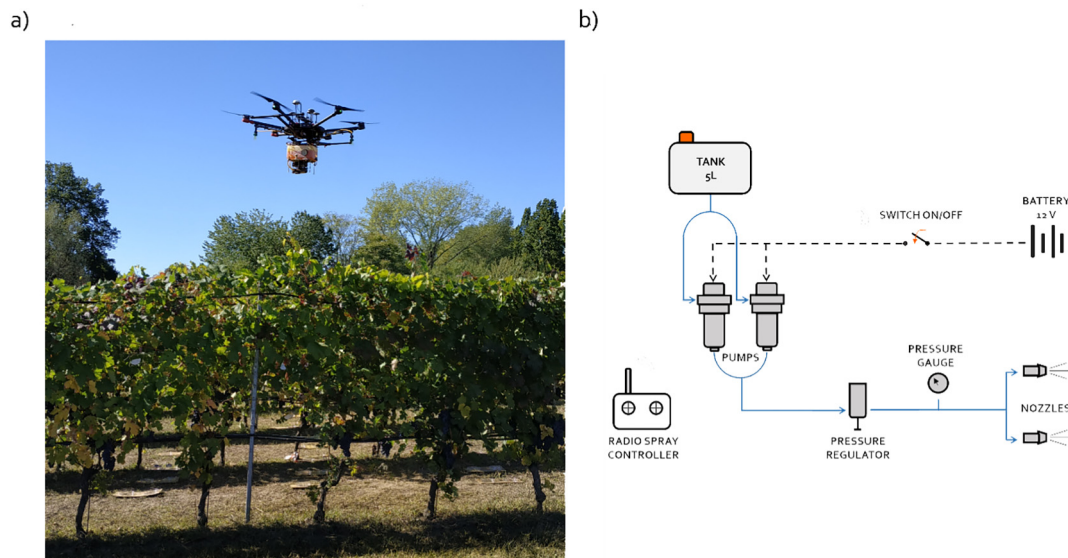
Fig. 1. a) UAV (Matrice 600 Pro, DJI) equipped with the customised sprayer system during a vineyard application, and b) schematic of the sprayer system circuit.

approaching the rotor axis. The velocity induced by the rotor decreases approximately up to a distance from the rotor plane equal to three times the diameter of the propeller area. Concerning the sprayer system, as shown in Fig. 1b, it consists of a 5 L polyethylene tank, two diaphragm pumps (Cybernova Pump, 70 W power, China), a manual pressure regulator (RS PRO, hydraulic flow control valve with a maximum flow rate of 20 L min^{-1}, United Kingdom), one vacuum pressure gauge (Hilitand, measuring range of 0–0.6 MPa, China), and two nozzle holders. On the bottom of the tank, the two pumps were assembled in parallel to guarantee the desired spray application rate at a stable pressure, and they were powered by an external battery 4S (1800 mAh, China) with two power regulators (Matek System, UBEC Duo, China). In addition, a remote-control system was included to turn the pumps on and off. The liquid pressure was controlled by a pressure regulator, manually set before the flight, and installed on the main pipeline at the outlet. A gauge, installed downstream, measured the pressure. Finally, two nozzle holders were installed on two of the six UAV arms to hold the nozzles under the rotors M2 and M5 at 910 mm from each other (Fig. 2a).

The nozzle holders were affixed perpendicularly to the rotors arm at 110 mm from the propellers axes, and oriented straight-down at 175 mm

from the rotors plane. It should be noted that the rotors plane is inclined at 7° with respect to the ground plane as detailed in Fig. 2b. The position of the nozzle holders relative to the UAV propellers was set according to the preliminary results of Bloise et al. (2021). The sprayer system weights 2.8 kg, excluding the liquid used in the experimental trials.

2.2. Experimental design

Twelve configurations were tested based on various combinations of different operating conditions: (i) three UAV flight modes, (ii) six nozzle types (three conventional three air inclusion), and (iii) two UAV cruise speeds.

Two different flight modes were used to fly the UAV across the vine rows either in one-way flights (named 1-way broadcast, Fig. 3a and Table 1) or in round-trip flights (named 2-way broadcast, Fig. 3b and Table 1). Basically, in testing the 2-way broadcast flight mode, the idea was to check the chance to cover the two sides of vineyard rows flying on the same route (round-trip flight) compared to the 1-way broadcast flight mode that foreseen a single pass with spray cloud impacting the row just from one side. A third flight mode was used to target the canopy which
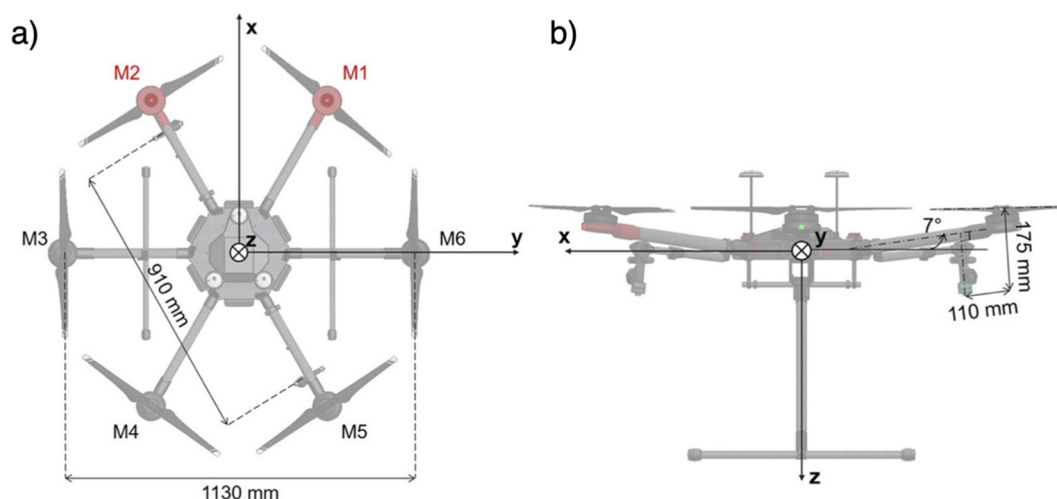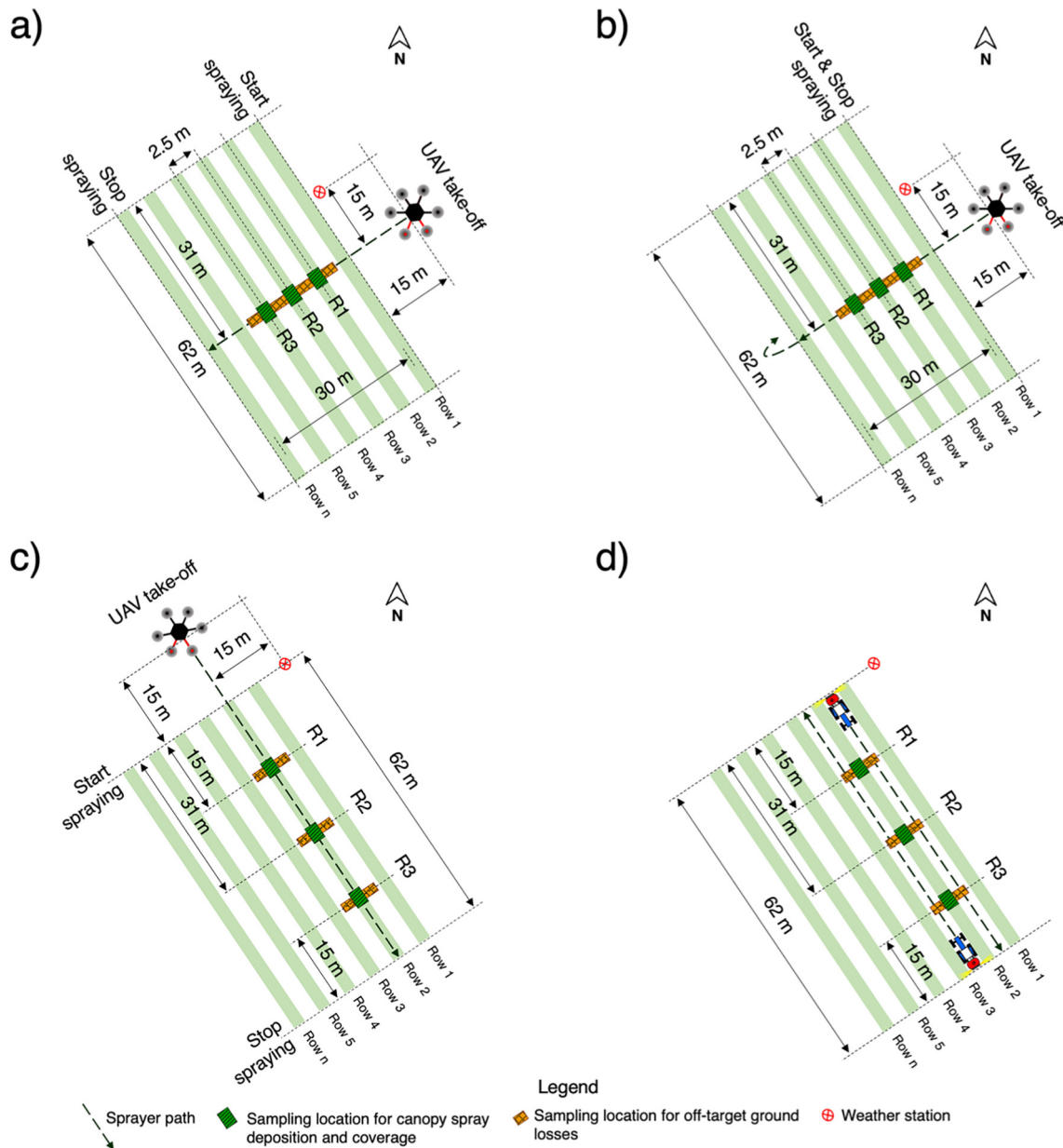

Fig. 2. Schematic of the adopted UAV-spray system with details about a) the rotors positions (aerial view) with the red rotors (M1 and M2) indicating the UAV nose, and b) the nozzle holders (lateral view).

Fig. 3. Schematic of the experimental layout with the adopted UAV flight modes: a) one-way across the row (1-way broadcast), b) round-trip across the row (2-way broadcast), and c) overhead flight along the vine row for a targeted spray application (1-way band). Layout and alley spray passages for d) the test performed by using the conventional airblast sprayer (reference spray application technique).

involved a single pass precisely above the vine row (named 1way-band, Fig. 3c and Table 1). All three flight modes were planned by using the UgCS drone mission planning and flight control software (SPH Engineering, Latvia). For the 1-way broadcast and 2-way broadcast flight modes, the UAV nose, represented with red rotors in Fig. 2a, was rotated (counterclockwise) by 60° with respect to the flight direction by using the UgCS software. This way, the UAV arms where the nozzle holders were installed were perpendicular to the flight direction and the spray swath was maximised when combined with flat fan nozzles. Contrary to the two flight modes for the broadcast spray application, in order to fly with the nozzles aligned with the vineyard row, the UAV nose was rotated by 30° with respect to the flight direction in the third flight mode. The two nozzles were aligned with the UAV flight to follow the vine row optimally. In all cases, the accuracy and precision were guaranteed by the installation of the D-RTK GNSS receiver (DJI, China) on the UAV.

The adopted nozzles were selected according to the three planned flight modes, and six different types were used (ASJ srl, Italy). Two types of flat fan nozzles, namely the conventional (SF 110 03 VP) and the Air Inclusion (AI) (AFC 110 03 VP) nozzles, characterised by a 110° spray angle and a rated volume flow rate between 0.85 and 1.83 L min^{-1} at 1.5–7 bar (blue colour, 03 size) (ISO, 2018), were used for the 1-way broadcast in field trials (Table 1). Also, for the 2-way broadcast trials, the conventional (SF 110 015 VP) and AI (AFC 110 015 VK) flat fan nozzles, characterised by a 110° spray angle and a rated volume flow rate between 0.42 and 0.92 L min^{-1} at 1.5–7 bar (green colour, 015 size) (ISO, 2018), were adopted. Finally, the conventional (HCI 60 03 VK) and AI (HCA 60 03 VK) hollow-cone nozzles, characterised by a 60° spray angle and a rated volume flow rate between 1.20 and 3.10 L min^{-1} at 3–20 bar (blue colour, 03 size) (ISO, 2018), were used for the 1-way band trials to target the spray as much as possible into the vines canopy. Different nozzle sizes were used in the 1-way broadcast and 2-way broadcast trials to maintain the spray application rate constant among the trials according to the UAV cruise speed. Indeed, two UAV cruise speeds (1 and 3 m s^{-1}) were selected to vary the spray application rate while the flight altitude was kept constant at 3 m above the ground

Table 1

Configurations of the adopted UAV-spray system and airblast sprayer for the in-field experimental trials.

Configuration	Flight height above the ground [m]	Treated area and passage mode	Nozzle model	N° of active nozzles	Working pressure [MPa]	Total liquid flow rate [L min^{-1}]	Cruise speed [m s^{-1}]	Spray application rate [μL per cm of travelled space]
T1	3 (aerial)	1-way broadcast	ASJ SF 110 03 VP	2	0.3	2.40	1.00	400
T2	3 (aerial)	1-way broadcast	ASJ SF 110 03 VP	2	0.3	2.40	3.00	133
T3	3 (aerial)	1-way broadcast	ASJ AFC 110 03 VK	2	0.3	2.40	1.00	400
T4	3 (aerial)	1-way broadcast	ASJ AFC 110 03 VK	2	0.3	2.40	3.00	133
T5	3 (aerial)	2-way broadcast	ASJ SF 110 015 VP	2	0.3	1.20	1.00	400
T6	3 (aerial)	2-way broadcast	ASJ SF 110 015 VP	2	0.3	1.20	3.00	133
T7	3 (aerial)	2-way broadcast	ASJ AFC 110 015 VK	2	0.3	1.20	1.00	400
T8	3 (aerial)	2-way broadcast	ASJ AFC 110 015 VK	2	0.3	1.20	3.00	133
T9	3 (aerial)	1-way band	ASJ HCI 60 03 VK	2	0.3	2.40	1.00	400
T10	3 (aerial)	1-way band	ASJ HCI 60 03 VK	2	0.3	2.40	3.00	133
T11	3 (aerial)	1-way band	ASJ HCA 60 03 VK	2	0.3	2.40	1.00	400
T12	3 (aerial)	1-way band	ASJ HCA 60 03 VK	2	0.3	2.40	3.00	133
T13	n/a	n/a	Albuz ATR 80 lilac VK	6	0.5	4.32	1.78	404[a]

n/a – not available (ground-based spray application).

[a] The spray application rate considers two passes (one per row side) of the airblast sprayer with only one side activated (6 nozzles).

in the entire set of in-field trials (Table 1). The spray pressure was maintained fixed at 0.3 MPa throughout the trials providing a total liquid flow rate of 1.2 and 2.4 L min^{-1} according to the nozzle sizes, 015 and 03 respectively (the two nozzles were always activated), thus resulting in a flow rate ranging between 133 and 400 μL per cm of UAV travelled space according to the UAV flight speed.

To compare the aerial spray application with a widespread and well documented spray application technique from the ground (Marucco et al., 2019), the Dragone Virgola airblast sprayer (Dragone Snc, Italy), designed ad hoc for vineyard spray applications, was used. The airblast sprayer was equipped with a 300 L polyethylene tank and six conventional double nozzle holders on each side. A conventional air conveyor with an axial fan (600 mm diameter) provides, on average, 19,000 m^3 h^{-1} at 540 rpm of tractor power take-off. For a broad comparison of the innovative UAV and traditional spray application techniques, six ATR 80 lilac hollow cone nozzles (Albuz® CoorsTek, France) were used at 0.5 MPa spray pressure, combined with a tractor forward speed equal to 1.78 m s^{-1} to obtain a very similar spray application rate between aerial and ground application (400 VS 404 μL per cm of tractor travelled space, Table 1). In particular, the spray application was carried out by activating only 6 nozzles on the sprayer side facing the vine row, with the sprayer passing in the two adjacent alleys of the selected vine row as detailed in Fig. 3d.

2.3. Experimental layout

The experimental layout was set up in the vineyard for simultaneous evaluation of canopy spray coverage and deposition, as well as in-field ground losses (Fig. 3). Measurements of the spray coverage and canopy deposition were taken at three locations along the UAV flight path (dark green squares in Fig. 3). The three sampling points along the row was used as replicates resulting in a sampling strategy broadly used by other authors in this research field (Gil and Escolà, 2009; Miranda-Fuentes et al., 2015). This allowed minimising environmental conditions variation among replicates thus making the data obtained broad comparable. The spray coverage was assessed at three heights (1.

bottom, 2. middle, 3. top) corresponding approximately to 0.7, 1.3, and 1.9 m height above the ground and at three depths (A. right edge, B. middle, C. left edge with respect to the UAV flight path) per vine canopy, as detailed by Grella et al. (2020a). At each sampling position, two paired Water Sensitive Papers (WSPs) (76 × 26 mm, Syngenta Crop Protection AG, Switzerland) were stapled to both leaf side, with an exposed surface of 19.76 cm^2 per leaf side. To assess spray deposition, filter paper discs of 120 mm diameter (90 g m^{-2}, Gruppo Cordenons SpA, Italy) were cut in two and then clipped adherent to each leaf side. In detail, the borders of the two half discs were coincident, thus maintaining the leaf in between hidden. Each half-disc represented a total exposed surface of 56.52 cm^2. This configuration of WSPs and filter papers in the canopy is broadly used to assess spray coverage (Hołownicki et al., 2002; Salyani et al., 2013; Rincón et al., 2020; Salcedo et al., 2020) and deposition (Nuyttens et al., 2004; Braekman et al., 2010; Miranda-Fuentes et al., 2016; Grella et al., 2020a) under real conditions during spray applications. Furthermore, in all trials, the artificial collectors were positioned in the same canopies and leaves thus avoiding the variability as the main objective was to identify the effect of different parameters tested minimising interferences from external factors. Measurements of the in-field ground losses were also taken using 140 mm diameter Petri dishes (APTACA SpA, Italy), which were aligned with the measuring positions in the canopy (orange rectangles in Fig. 3). Different sampling locations were therefore selected for the evaluation of ground losses by adapting the layout detailed by Grella et al. (2020a), namely i) under the canopy of the sprayed vines, ii) in the middle of each inter-row, and iii) between these two last positions. In each location, two paired Petri dishes (total exposed surface of 307.72 cm^2) were affixed to wooden boards placed directly on the ground to withstand the UAV rotor downwash.

The sampled vines were distributed within the experimental plot as shown in Fig. 3. The UAV take-off point was set 15 m away from the vineyard and in front of it, and the spray application started at the entrance of the vineyard. A Stonex S900A GNSS receiver (STONEX® srl, Italy) was used to acquire the position of the waypoints, thus aligning the UAV flight

path in parallel with the vine rows when the 1-way band spray application was carried out and perpendicularly to the vine rows in the broadcast modes to pass exactly above the sapling locations as described in § 2.2.

The experimental plot reported in Fig. 3d was used to measure canopy coverage and deposition when the airblast sprayer was used as the reference spray application technique. In this case, the two inter-rows adjacent to the second row of the vineyard were used for the sprayer track and the in-field ground losses were sampled in two locations instead of three, namely inter-row and under the vines (Grella et al., 2020a), to allow for the tractor passage.

2.4. Field test location and vineyard characteristics

The field trials were carried out in a vertical shoot position trellised vineyard (cv. Barbera) at growth stage BBCH 89 "Berries ripe for harvest" (Lorenz et al., 1995) located at the DiSAFA facilities in Grugliasco (Turin, Italy). The grapevines were spaced at 2.5 m and 0.8 m between and within rows respectively, thus resulting in a density of about 5000 vines per hectare. Furthermore, the rows were 62 m long with a northwest-southeast orientation, and 146° azimuth. To check for possible variability between the selected vines for the spray canopy deposition and coverage measurements, the canopies were characterised by using the inclined point quadrat technique as originally proposed by Wilson (1963) and recently used by other authors to characterise 3D crops (Vitali et al., 2013; Palleja and Landers, 2017; Grella et al., 2019). Block PQT (Point Quadrat Technique) measurements were set up, consisting of a 3 m row length where the PQT measurements were taken in the vegetative strip at heights between 0.4 and 2.2 m. The average vineyard height from the ground was 2.21 m with a vegetative strip of 1.68 m and a canopy width of 0.55 m. Based on the PQT measurements, the mean vegetative parameters were calculated according to Pergher and Petris (2008) and resulted in average in 2.6 leaf layers and 15.7 % gaps; it follows that the Leaf Area Index (LAI) ranged between 1.5 and 1.9 (non-dimensional). Therefore, the grapevine canopies selected for sampling did not vary substantially among each other and are representative of modern commercial vineyards where LAI below 2.5 must be ensured through adequate canopy management techniques such as shoot trimming, positioning, and tying (Intrieri and Poni, 1995).

2.5. Environmental conditions monitoring

A weather station was employed to monitor the relevant environmental conditions over the full duration of the trials. The weather station was positioned 15 m away from the UAV flight path in a crop-free area (crossed red circle in Fig. 3). The weather station was equipped with a sonic anemometer 232 (Campbell Scientific, USA) at a 4.0 m height to measure wind speed and direction, and two thermo-hygrometer HC2S3 probes (Campbell Scientific, USA) placed at 2.0 and 4.0 m heights to measure the air temperature and relative humidity (RH). All measurements were taken at a frequency of 0.1 Hz and all data was recorded automatically by a CR800 data logger (Campbell Scientific, USA). The average air temperature and RH ranged between 15.0 and 15.9 °C, and 23.6 and 71.1 % respectively, while the average wind speed recorded in each trial was always below 1.53 m s^{-1}. The weather featured optimal conditions for spray applications as defined by the Best Management Practices (BMPs) (TOPPS-Prowadis Project, 2014). In all cases, the experimental trials were conducted in "light air" conditions (Barua, 2005), making the data derived from the different trials broadly comparable. The weather data recorded during the trials for each configuration is shown in the Appendix (Table A1). Noteworthy, under real field conditions spray applications are largely carried out when the wind speeds are higher than 1.5 m s^{-1} with possible effects on both canopy deposition and off-target losses, especially those related to the spray drift (Wang et al., 2021).

2.6. Droplet size spectra characteristics

The droplet size spectra produced by the adopted nozzles, both conventional and AI, were determined through laboratory measurements, conducted at the DiSAFA facilities in Grugliasco (Turin, Italy), by using a Malvern Spraytec laser diffraction system STP5342 (Malvern Instruments Ltd., UK). The methodology used was like the one described in Grella et al. (2020b) for pneumatic nozzles; the main difference consists in the absence of an airflow rate generated by a tangential fan during the laser measurements, as it is not necessary for the liquid atomisation when using hydraulic nozzles. The liquid pressure, and thus the liquid flow rate, adopted in the laboratory trials were the same as the one used in the field trials (Table 2).

The droplet diameter corresponding to 10th (D[v,0.1]), 50th or Volume Median Diameter (VMD) (D[v,0.5]), and 90th (D[v,0.9]) percentiles of spray liquid volume was determined for each nozzle. Additionally, the % of spray liquid volume generated with droplet diameters smaller than 100 μm was calculated and reported in Table 2 as V100 for its relationship with droplet drift ability. Several authors have explained the relation between the drift and the droplet size linked to the V100 indicator (Nuyttens et al., 2007; Baetens et al., 2008; Arvidsson et al., 2011; Gil et al., 2015; Grella et al., 2020b). For each nozzle type, two nozzles were randomly sampled from a batch, and three measurements were performed for each nozzle. The two nozzles used for the laboratory trials were then mounted on the UAV spray system and used for the field trials. The same procedure was also adopted for charactering the nozzles mounted on the airblast sprayer used as a reference in the field trials. After measuring the droplet size spectra, in order to install six nozzles per sprayer side, two nozzles were mounted together with the other nozzles belonging to the batch from which the tested nozzles were selected.

2.7. Sprayed mixture and tracer concentration

To evaluate spray deposits on the collectors, a solution of water and E-102 Tartrazine yellow dye tracer (85 % *w*/w) (Novema srl, Italy), at a

Table 2
Droplet size spectra and main parameters of the nozzles used in the field trials.

Nozzle model	Nozzle type	Nozzle technology	Working pressure [MPa]	Flow rate [L min^{-1}]	D [v,0.1][a] [μm]	D [v,0.5][a] [μm]	D [v,0.9][a] [μm]	V$_{100}$[b] [%]	Spray classification[c]
ASJ SF 110 03 VP	Flat fan	Conventional	0.3	1.20	77	159	313	25	Medium
ASJ AFC 110 03 VK	Flat fan	Air inclusion	0.3	1.20	121	306	669	8	Coarse
ASJ SF 110 015 VP	Flat fan	Conventional	0.3	0.60	70	140	265	31	Fine
ASJ AFC 110 015 VK	Flat fan	Air inclusion	0.3	0.60	128	298	646	6	Coarse
ASJ HCI 60 03 VK	Hollow cone	Conventional	0.3	1.20	67	145	281	31	Fine
ASJ HCA 60 03 VK	Hollow cone	Air inclusion	0.3	1.20	203	597	1238	3	Extra coarse
Albuz ATR 80 lilac VK	Hollow cone	Conventional	0.5	0.36	54	100	171	58	Fine

[a] 10 % of the spray liquid volume fraction is made up of droplets smaller than D[v,0.1]; D[v,0.5] is the volume median diameter; 90 % of the spray liquid volume is made up of droplets smaller than D[v,0.9].

[b] V$_{100}$: spray liquid fraction generated with droplets smaller than 100 μm.

[c] ASABE S572.1, Spray nozzle classification by droplet spectra (ASABE, 2009).

concentration of about 10 g L^{-1}, was added to the UAV spray system tank. Tartrazine was chosen as a tracer for its high extractability and low degradation. Prior to each application, a blank procedure was carried out by placing two Petri dishes and two filter papers in the experimental area and collecting those 30 s before spraying started. Also, sprayed liquid samples were collected from the spray tank at the nozzle outlet, before and after spraying, to ascertain the precise tracer concentration for each trial.

2.7.1. Spray deposit quantification

The adopted collectors in the trials were washed with deionised water to extract the tracer. A volume of 30 mL of deionised water was added into the sealed bags containing the filter papers used in the canopy, which were then shaken for 5 min and left soaking for another 55 min. Meanwhile, 10 mL of deionised water were added in the Petri dishes and shaken for 3 min to completely extract and homogenise the washing solution.

The Tartrazine concentration was determined by measuring the absorbance of the washing solution with a UV-1600PC VWR spectrophotometer (VWR International, USA), set to 427 nm wavelength for peak absorption of the Tartrazine dye, and by comparing the results against a calibration curve obtained in the laboratory before the beginning of the analysis. A further dilution of the washing solution was necessary when the Tartrazine concentration was too high for the optimal reading range of the spectrophotometer. In all cases (filter papers and Petri dishes), three absorbance measurements were taken for each sample.

The spray deposit on each Petri dish $\left(\mathcal{D}_i^{pd}\right)$ and filter paper $\left(\mathcal{D}_i^{fp}\right)$ in [μL cm^{-2}] was calculated according to the following Equations

$$\mathcal{D}_i^{pd} = \frac{\left(p_{smpl} - p_{blk}\right) \times \mathcal{V}}{0.5 \times \left(p_0 + p_{end}\right) \times \mathcal{A}_{col}} \tag{1}$$

and

$$\mathcal{D}_i^{fp} = \frac{\mathcal{D}_i^{pd}}{\varepsilon} \tag{2}$$

where p_{smpl} is the measured absorbance of the sample (dimensionless), p_{blk} is the measured absorbance of the blank (dimensionless), $\mathcal{V}$ is the volume [μL] of the dilution liquid (deionised water) used to extract the tracer deposit from the collectors, p_0 is the absorbance value of the spray mix concentration sampled at the nozzle outlet just before each trial (dimensionless), p_{end} is the absorbance value of the spray mix concentration sampled at the nozzle outlet at the end of each trial (dimensionless), $\mathcal{A}_{col}$ is the area of the collector exposed to the spray [cm^2], and ε is the extractability factor equal to 0.589 according to Miranda-Fuentes et al. (2016).

Since different spray application rates were applied according to the tested UAV cruise speeds, the collectors' deposit $\mathcal{D}_i$ was standardised in order to compare the twelve different tested configurations (Llorens et al., 2010). The standardised deposition $\mathcal{D}_{i,std}$ [μL cm^{-2}] was calculated as follows

$$\mathcal{D}_{i,std} = \frac{\mathcal{D}_i \times \theta_{std}}{\theta_{appl}} \tag{3}$$

where $\mathcal{D}_i$ is the spray deposit on a single collector [μL cm^{-2}] as calculated in Eqs. (1)–(2), θ_{std} is the applied spray application rate used for data standardization, equal to 250 and expressed in μL per cm of travelled space, and θ_{appl} is the spray application rate effectively applied during the field trials and expressed in μL per cm of travelled space.

2.8. Images analysis for spray coverage characterisation

The collected WSPs were scanned at 600-dpi resolution using an HP Colour LaserJet Pro MPF M479dw printer with an integrated scanner. The scanned WSPs were then analysed by using a specific image processing

macro (Zhu et al., 2011; Miranda-Fuentes et al., 2016) developed in the ImageJ software (National Institutes of Health, USA). The spray coverage [%] was calculated as the ratio between the spray deposits area (area covered by stains) and the total area effectively analysed on the WSPs, while the deposits density (n° of stains per cm^2) was determined as the number of spray deposit stains per WSP target area unit (Fox et al., 2003; Cerruto et al., 2019).

2.9. Statistical and data analysis

The canopy and ground deposit data was analysed by using linear mixed effect models in the R environment (R Core Team, 2021) with the *lme* function included in the *nlme* package (Pinheiro et al., 2021). Before the analysis, the canopy and group deposit values were standardised (z-score) and the values > |3| were excluded as considered to be outliers.

The statistical analysis was divided into two steps. First, the UAV flight mode, nozzle type, and UAV cruise speed were considered as fixed factors to assess their effect on the canopy and ground deposits and to identify which UAV flight mode maximised the canopy deposit. Second, the canopy height (the positions at which the filter papers were placed in the canopy), nozzle type, and UAV cruise speed were specified as fixed factors for evaluating their effect on the canopy deposit only for the best UAV flight mode. Regarding the effects on ground the deposit for the best UAV flight mode, the distance (the positions at which the Petri dishes were placed on the ground), nozzle type, and UAV cruise speed were used as fixed factors. In all these models, the two- and three-way interactions were included, and the three replicates (Fig. 3) were considered as random factors to account for spatial autocorrelation. The assumptions of homogeneity of variances, normality and independence of the residuals were graphically checked. As the model residuals were often affected by heteroscedasticity, a weighting function was used to correct the variances in each model and the assumptions were checked again. This variance correction was carried out through the argument *varIdent* in the *lme* function by setting as a grouping variable the factor for which the heterogeneity of residuals variance was detected. After the assessment of the significance of the fixed and interacting factors in each model (*join_tests* function, *emmeans* package – Russell, 2021), Tukey's post-hoc tests with Bonferroni-adjusted *p*-values (*join_tests* function, *emmeans* package – Russell, 2021) were performed for the significant factors. The significance threshold was set to 0.05.

The spray coverage data, obtained by WSP image analysis, was evaluated in order to investigate the suitability of the tested UAV spray configurations in terms of the expected efficacy of the spray application according to the possible treatment specifications, i.e. insecticide or fungicide. Therefore, the thresholds for over-spray and stains per cm^2, provided by Syngenta Crop Protection AG, were used as a reference (Chen et al., 2013; Miranda-Fuentes et al., 2015; Salcedo et al., 2020; Grella et al., 2022b). The over-spray was defined as any situation with a spray coverage >30 %, while the insecticide and fungicide applications could be considered effective when a deposit density higher than 30 and 70 stains per cm^2 was obtained, respectively. Therefore, the percentage of WSPs that meet both criteria, namely not over-sprayed and characterised by a deposit density higher than the defined stain thresholds, were calculated. Based on the above-described data analysis, the best UAV-spray configuration for vineyard spray applications was identified, among those tested, and compared to the airblast sprayer used as the reference technique for vineyard spray applications. In particular, the canopy deposition, coverage, and off-target ground losses obtained by the best UAV-spray configuration were compared to the airblast sprayer for a better and complete understanding of the spray efficiency reached by the innovative UAV-spray application technique.

3. Results and discussion

Regarding the procedure used for the data analysis, first the statistical analysis of both the canopy and ground deposits data is reported and discussed. Second, the comparison of the best UAV-spray system configuration

with a traditional airblast sprayer is presented. Finally, the best UAV spray configuration, chosen according to the obtained results, was compared to a conventional airblast spray application (ground-based reference spray application technique).

3.1. Canopy deposit

Based on 639 valid samples (9 data were removed as outliers), the canopy spray deposit values obtained in the experimental trials were in the range of 0 to 0.861 µL cm^{-2}, and they proved to be statistically different according to the adopted UAV-sprayer system configurations as shown in Table 3.

The interaction between nozzle type and UAV cruise speed was found significant, thus affecting the canopy deposit (Table 3). In particular, the standardised average canopy deposition ranged from 0.059 µL cm^{-2} when using AI nozzles to 0.128 µL cm^{-2} when using conventional nozzles, when both operated at a 3 m s^{-1} UAV cruise speed (Fig. 4). Intermediate values were found for the conventional and AI nozzles operated at a 1 m s^{-1} cruise speed. However, the post-hoc test detected no statistical differences in the canopy deposit between the nozzle types when the UAV cruise speed was 1 m s^{-1}. Meanwhile, significant differences among the nozzle types were detected when both were used at 3 m s^{-1}, showing that the canopy spray deposition for conventional nozzles doubled compared to those obtained with AI nozzles (Fig. 4). Furthermore, a different trend was noticed for canopy spray deposition at increasing UAV cruise speed, depending on the nozzle type. For conventional nozzles, increasing the UAV speed resulted in significant spray deposition increase, while the UAV cruise speed did not have any effect on the canopy deposit when using the AI nozzles. The numerical analyses and validations performed by Wen et al. (2019) when using a quad-rotor UAV showed how cruise speed and altitude cause a horseshoe vortex in the downwash flow field, which leads to the entrainment of the droplets. More recently, Wang et al. (2021) based their numerical simulations on the data collected in wind tunnel experiments when using a DJI Matrice 600 Pro (the same UAV used in our study), indicating a cruise speed of 4 m s^{-1} and a flight height of 2.5 m as optimal parameters for UAV-spray applications. Wang et al. (2021) suggested a high cruise speed, among those tested between 1 and 4 m s^{-1}, since with an increase of flight speed and height, the backward tilt angle of the downwash airflow field gradually increases, and the length and width of the longitudinal and horizontal spread on the ground decreases. Besides, at 3 m the vortices on both sides of the fuselage gradually become larger and gather towards each other, which entrains and affect the spatial movement and distribution of the droplets. This phenomenon is accentuated when using conventional nozzles with a small orifice size, as used in our experimental trials (Table 2), as their droplets are fine and thus diverted from their original trajectory by the downwash flow field. Indeed, it is well known that when using conventional airblast sprayers, the sprayed droplets follow the direction of the fan airflow, thus conveying the sprayed liquid into the canopy (Dekeyser et al., 2013); similarly, the downwash generated
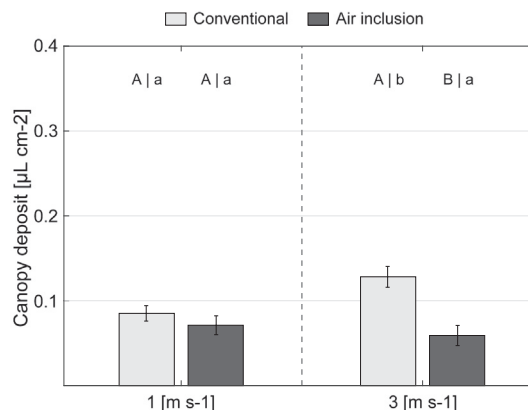

Fig. 4. Average spray canopy deposit values [µL cm^{-2}] for different nozzle types (conventional and air inclusion) and UAV cruise speeds (1 and 3 m s^{-1}). Different uppercase letters indicate significant differences between nozzle types per UAV cruise speed, whereas lowercase letters indicate significant differences between UAV cruise speeds per nozzle type. The differences are defined according to Tukey's post hoc tests with Bonferroni-adjusted p-values ($p < 0.05$). The error bars represent the standard error of the means.

by the UAV rotors can be used for the same purpose, increasing the chances of reaching the innermost canopy parts. In conclusion, the higher the turbulence of the downwash, the higher the possibility is for the droplets to penetrate the canopy, especially for the fine ones. The behaviour of the downwash flow field described by Wang et al. (2021) can well represent the one generated by the UAV during our experimental trials where, irrespective of the flight modes tested, the combination of a 3 m s^{-1} cruise speed and conventional nozzles at a 3 m flight height, resulted in a suspended turbulent fine spray cloud able to envelope the vines canopy and better penetrate it. On the contrary, when the AI nozzles were used, the coarse spray generated (Table 2) was less sensitive to the horseshoe-shaped eddy current in the downwash flow field, whose turbulence at higher UAV cruise speeds helps in driving the fine droplets into the canopy. Furthermore, according to the results reported by Wang et al. (2021), if the UAV-spray application in conditions of severe crosswind (higher than 3 m s^{-1}) cannot be avoided, the selection of the AI nozzles can represent the best choice as the spray drift is reduced by up to 95 % and the canopy spray deposition is increased in the artificial vineyard. In our study, the AI nozzles showed the worst spray performances when tested under real field conditions. Indeed, in windy conditions, the fine droplets can be diverted and blown away from the sprayed area by environmental wind before reaching the target, thus giving worse results concerning the canopy spray deposition. In light air conditions, our experimental results underlined how the conventional nozzles can represent the best choice also for UAV-spray applications. For this reason, similarly to the conventional spray applications, the proper selection of nozzle types, and therefore the droplet size spectra it generated, has to be taken into account according to the crop and environmental conditions at the time of application, thus maximising canopy deposition and, at the same time, minimising spray drift losses.

According to the results reported in Table 3, the flight mode also exerted an effect on the canopy spray deposition amount, with significant interaction with the nozzle type. Indeed, as shown in Fig. 5, a higher canopy spray deposit amount (0.237 µL·cm^{-2}) was obtained by using the conventional nozzles in combination with the 1-way band flight mode (flight above the canopy, see Fig. 3), compared to the deposit amount obtained when testing the AI nozzles. No statistical differences were noticed among the AI nozzles used in combination with the different flight modes (Fig. 5). Also, there was no difference between the conventional and AI nozzles in both broadcast flight modes (1-way and 2-way). The results indicated that during the UAV spray application, the strategy of flying above the canopy to match as much as possible the canopy presence and its

Table 3
Results of the linear mixed model ($p < 0.05$) for the canopy spray deposition [µL cm^{-2}].

Model term	DF1	F ratio	p value[a]
Main effects			
Flight mode	1	2.390	0.1226 [NS]
Nozzle type	1	18.089	<0.0001 ***
UAV speed	2	42.886	<0.0001 ***
Interactions			
Nozzle x Speed	1	7.662	0.0058 **
Nozzle x Flight	2	24.830	<0.0001 ***
Speed x Flight	2	1.919	0.1476 [NS]
Nozzle x Speed x Flight	2	2.078	0.1261 [NS]

DF2 = 625.
[a] Statistical significance level: NS $p > 0.05$, * $p < 0.05$, ** $p < 0.01$, *** $p < 0.001$.
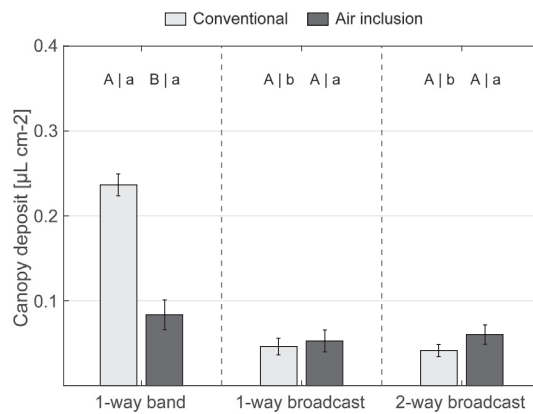
Fig. 5. Average canopy deposit values [μL cm^{-2}] for different nozzle types (conventional and air inclusion) and UAV flight modes (1-way band, 1-way and 2-way broadcast). Different uppercase letters indicate significant differences between nozzle types per UAV flight mode whereas lowercase letters indicate significant differences between UAV flight modes per nozzle type. The differences are defined according to Tukey's post hoc tests with Bonferroni-adjusted *p*-values ($p < 0.05$). The error bars represent the standard error of the means.

projected surface onto the ground with the sprayed liquid can be a reliable way to increase the overall canopy deposition using conventional nozzles. Moreover, even if the canopy deposit measured for the 1-way band flight mode using the AI nozzles was not significantly higher than those measured for other broadcast flight modes, an increasing trend is noticeable suggesting the target application has been more effective than others even using the AI nozzles (Fig. 5). These results contrast with those found by Giles and Billing (2015), who performed vineyard spray applications and suggested the cross-flight to the vine rows orientation as the best flight mode to improve canopy deposition. However, a helicopter was used without optimising the spray application when the UAV flew along the row orientation; indeed, Giles and Billing (2015) provided a broadcast application even flying along the row orientation. Sarri et al. (2019) tested a multi-rotor UAV in a high slope terraced vineyard performing a broadcast spray application by flying perpendicular with respect to the vine rows orientation. The authors obtained no differences between the conventional and AI nozzles on the droplet coverage when using WSPs placed at different positions in the canopy. To the best of our knowledge, in the literature, no one has investigated the possibility of carrying out targeted vineyard spray applications by using UAV-spray systems. Based on our results, this can represent a successful strategy for UAV-spray applications in vineyards, especially considering the principle of precision agriculture that, in general, advises against broadcast spray applications. Furthermore, our results are consistent with what is reported by Meng et al. (2020) regarding peach trees, where the authors claimed that the UAV flight mode plays a key role during spray applications and must be defined according to both the tree shape and the spray system features. In this regard, in our experimental trials for the band-spray application, the UAV flight mode was customised to follow exactly the vine rows to be sprayed with two hollow cone nozzles characterised by a 60° spray angle, thus reducing the spray pattern (Table 1).

To visualise how the spray deposit was distributed in the different canopy portions, a colour map for each UAV-sprayer configuration is reported in Fig. 6, where the data is also split by leaf side (upper and lower). In general, Fig. 6 further underlines how, in the broadcast spray application (1-way or 2-way flight modes), a very limited amount of canopy deposition was measured in most canopy positions (some equal to zero), especially for the bottom and middle positions irrespective of canopy depth (A, B or C) and leaf sides. With the broadcast flight modes, a limited amount of deposit was measured only on the top part of the canopy. Focusing on the 1-way band flight mode, the results were different from those described for the broadcast flight modes. The spray deposit obtained when using the AI nozzles was almost absent in the bottom part of the canopy. The

spray deposit slightly increased in the middle part, but, in general, it was lower than the canopy spray deposition obtained when using conventional nozzles. Indeed, the 1-way band flight mode, combined with the other parameters, allowed an increased canopy deposit penetration, especially at the bottom and middle canopy heights, resulting in benefits for the canopy spray uniformity in all canopy positions (Fig. 6). This task is not easy to accomplish even with conventional airblast sprayers (Grella et al., 2022b). Concerning the canopy depth, namely the A, B and C positions, a specific trend according to the tested parameters was not observed.

3.2. Canopy coverage

The relationship between covered surface (%) and deposit density (n° of stains per cm^2) is reported in Fig. 7 for each tested UAV-spray system configuration. In line with Chen et al. (2013), WSPs with a coverage higher than 30 % (vertical dashed lines in Fig. 7) were classified as over-sprayed, thus considering that a high coverage does not necessarily imply a more effective spray application (Garcerá et al., 2011). Thresholds of 30 and 70 stains per cm^2 (horizontal dashed lines in Fig. 7) were used to evaluate the deposit density for effective insecticide and fungicide applications, respectively (Zhu et al., 2011; Salcedo et al., 2020). The scatter plots in Fig. 7 underline a completely different situation compared to those usually found when using conventional airblast sprayers in vineyard applications. Indeed, only two cases (1-way band flight mode combined with a 1 m s^{-1} UAV cruise speed and the two tested nozzle types) showed 3.7 % of the WSPs as characterised by an over-spray situation (WSP coverage higher than 30 %). While it is fine not to over-spray because an increase in the application rate might not involve an increment in the biological efficacy of the PPP (TOPPS-Prowadis Project, 2014), on the other hand Fig. 7 underlines what a few WSPs can accomplish with the deposit density thresholds for an effective insecticide or fungicide spray application, underlying a general under-spray occurrence irrespective of the adopted configuration. For example, in the worst case, when using the AI nozzles at 3 m s^{-1}, regardless of the UAV flight mode, 100 % of the WSPs were under-sprayed. When using an airblast sprayer, equipped with conventional nozzles, >35 % of the WSPs are usually characterised by a deposit density higher than 70 stains per cm^2 when a spray application rate equal or higher than 90 L ha^{-1} was applied (Grella et al., 2022b).

Even if the obtained canopy spray coverage is lower than expected for a good spray application of fungicide or insecticide, the results strongly support the data previously discussed about the canopy spray deposit and ground losses. Indeed, the best canopy coverage was found when the 1-way band UAV-spray application was carried out with the conventional and AI nozzles. The results showed that 74.1 and 75.9 % of the WSPs were under-sprayed for insecticide applications and that 92.6 and 96.3 % of the WSPs were under-sprayed for fungicide applications, respectively (Fig. 7). In general, the low cruise speed showed better results as the applied liquid rate was three times higher than the one applied at 3 m s^{-1}. While the canopy spray deposition values were standardised to the same application rate for a broad comparison of the tested parameters, the standardization of the WSPs spray coverage parameters to the same spray application rate is not a reliable procedure due to the spots touching or overlapping (Fox et al., 2003; Grella et al., 2019 and 2022b). When increasing the spray application rate, the stains overlap becomes more considerable, thus resulting in a flattening of the deposit density. In this way, the spray coverage results also made it possible to investigate the effects of the spray application rate on the canopy spray deposition. As a final remark, it can be noted that for UAV-spray applications in vineyards at full growth stage, the spray application rate should be increased in comparison with those tested in this experimental work in order to possibly increase the spray coverage and therefore the deposit density. Similarly, in addition to the research done by Li et al. (2021), further trials are needed to better understand the most suitable spray application rate for UAV-spray applications in vineyards in order to guarantee an adequate treatment efficacy, also according to the different growth stages that are characterised by a different canopy density and shape. However, for a comprehensive evaluation,
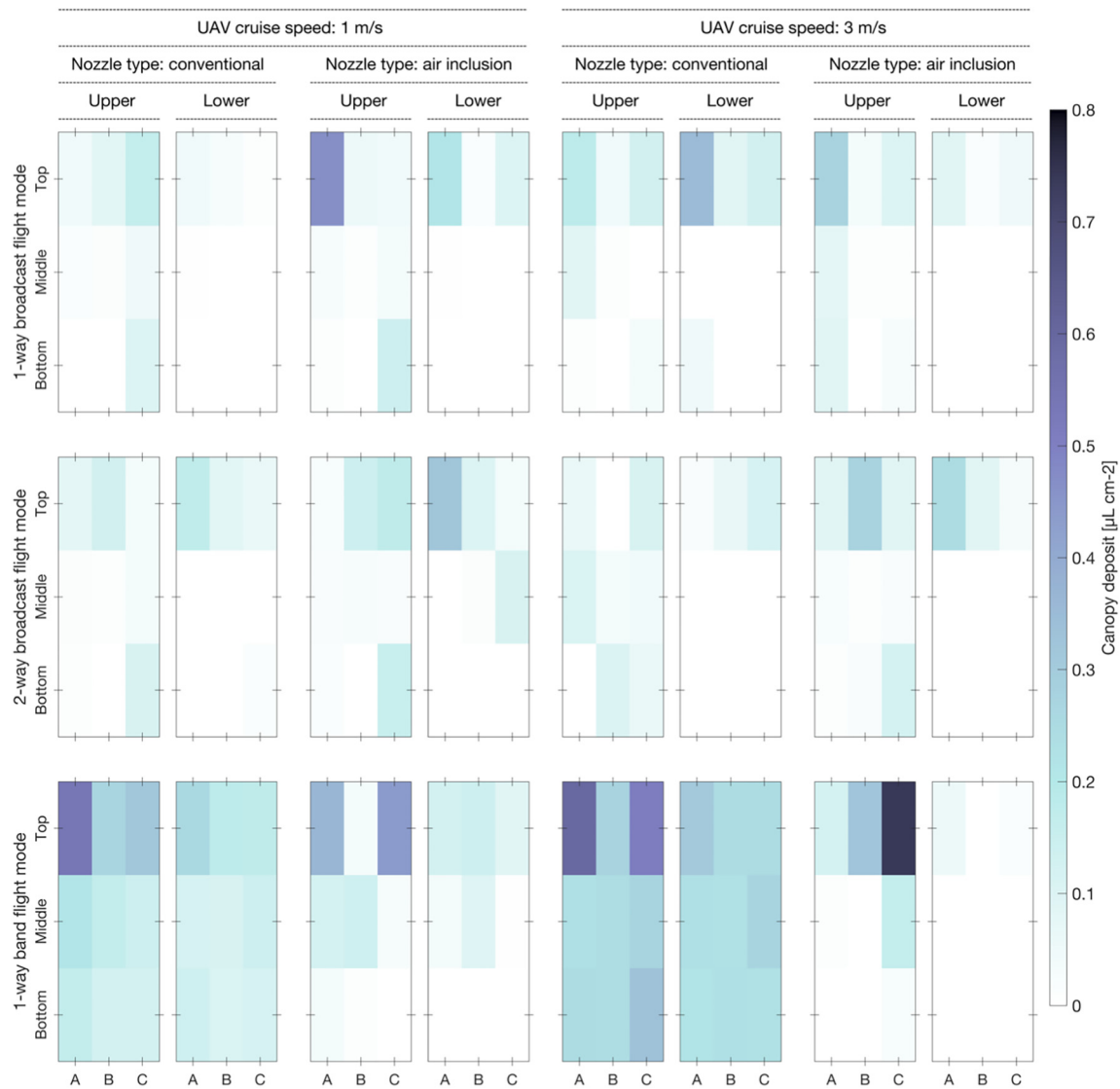
Fig. 6. Colour maps representing the distribution of the canopy spray deposits [$\mu L\ cm^{-2}$] according to: (i) UAV cruise speed (1 and 3 m s^{-1}), (ii) nozzle types (conventional and air inclusion), (iii) flight mode (1-way and 2-way broadcast, and 1-way band), (iv) canopy height (bottom, middle and top), (v) upper and lower leaf sides, and(vi) canopy depth (A, B and C).

ad hoc trials are needed in order to evaluate the biological efficacy of the spray applications that use UAV-spray systems, and to date no published research in 3D crops has been found, at least regarding vineyard crops.

3.3. Ground deposit

The in-field spray ground losses deposit values, obtained from 360 valid samples collected in the field trials, showed a range of none and 1.464 μL cm^{-2}, and were found to be statistically different according to the adopted working parameters as shown in Table 4.

Ground losses were significantly affected by the nozzle types and the UAV cruise speed, which showed a significant interaction (Table 4). Fig. 8 shows the average ground losses according to the UAV cruise speed for the two nozzle types. It can be noticed that the effect of the nozzle type on the ground losses was significative both at the 1 and 3 m s^{-1} UAV cruise speeds but with a different trend. Indeed, at the speed of 1 m s^{-1}, the conventional nozzles caused higher spray losses than the AI nozzles (+ 18 % on average). On the contrary, the ground losses for the conventional nozzles were much lower (− 47 % on average) than the AI nozzles when the UAV cruise speed was set at 3 m s^{-1}. Concurrently, the ground

losses were not affected by the UAV cruise speed (1 or 3 m s^{-1}) in combination with AI nozzles, while the higher the UAV speed, the lower the ground deposit was for the conventional nozzles. These results agree with those shown in Fig. 4, where higher amount of canopy spray deposition can be observed for the conventional nozzles combined with the 3 m s^{-1} of UAV cruise speed. Indeed, according to the spray mass balance approach widely used to calculate and evaluate spray application efficiency (Jensen and Olesen, 2014), generally, the higher the spray amount found in the canopy is, the lower the amount of spray losses, both in the case of in-field and spray drift ground losses. In our study, which is focused on the optimisation of canopy spray deposition, only the in-field ground losses were measured, while the spray drift losses can be considered very low compared to the other measured spray fractions as the trials were conducted in light air (Table A1). Spray drift, usually measured according to the ISO 22866 standardised methodology, requires intense wind speed to obtain reliable results as presented by Wang et al. (2021). To the best of our knowledge no other author has measured the ground deposit within the inter rows of the vineyard. Wang et al. (2021), focusing their trials on the measurements of the UAV spray drift, measured the sedimentation at ground level and the airborne drift in the downwind area outside the artificial vineyard. Even if
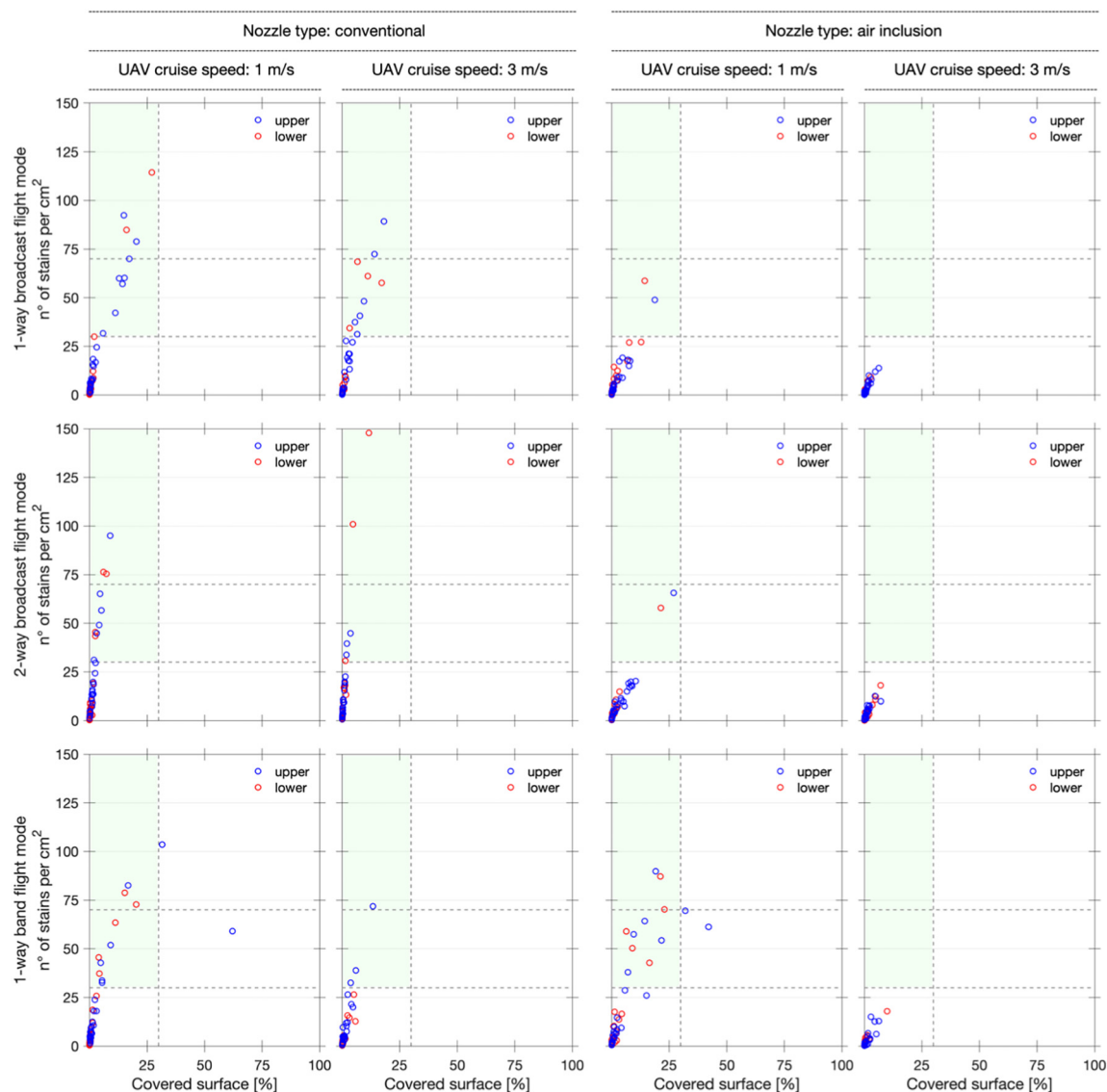
Fig. 7. Plots of spray coverage (%) and deposit density (n° of stains per cm²) for the different configurations tested: (i) nozzle type (conventional and air inclusion), (ii) UAV cruise speed (1 and 3 m s⁻¹), and (iii) UAV flight mode (1-way and 2-way broadcast, and 1-way band). Different colours represent the data split by upper and lower leaf sides. Horizontal dashed lines represent the deposit density thresholds for effective insecticide (30 stains per cm²) and fungicide (70 stains per cm²) applications, respectively. The vertical dashed line represents the spray coverage threshold for the over-spray situation (30 %). The thresholds were recommended by Syngenta Crop Protection AG.

it is well known that spray drift is one of the major concerns related to the environmental contamination risk during spray applications, the in-field spray losses can represent a huge environmental risk in relation to the

Table 4
Results of the linear mixed model ($p < 0.05$) for the in-field ground losses deposition [µL cm⁻²].

| Model term	DF1	F.ratio	p value [a]
Main effects			
Flight mode	1	35.736	<0.0001 ***
Nozzle type	1	4.607	0.0325 *
UAV speed	2	44.377	<0.0001 ***
Interactions			
Nozzle x Speed	1	25.564	<0.0001 ***
Nozzle x Flight	2	11.022	<0.0001 ***
Speed x Flight	2	5.804	0.0033 **
Nozzle x Speed x Flight	2	1.586	0.2062 NS

DF2 = 346.
[a] Statistical significance level: NS $p > 0.05$; * $p < 0.05$; ** $p < 0.01$; *** $p < 0.001$.

run-off and leaching phenomenon (Kellogg et al., 2002; Schriever et al., 2007; Vymazal and Březinová, 2015). Indeed, our results underline that during UAV-spray applications, the in-field ground losses can, on average, be five times higher than the spray deposits measured on the canopies (Figs. 4–6). This phenomenon is still not well investigated and reported in the literature, especially for UAV-spray applications.

In this respect, the significant effect of the UAV flight mode on the ground losses is of particular interest, where the values for the 1-way band (0.246 µL cm⁻²) were on average 55 % lower than those in the 1-way broadcast (0.53 µL cm⁻²) and 2-way broadcast (0.558 µL cm⁻²) flight modes (Fig. 9). Indeed, in the literature, other authors have reported results only about broadcast spray applications for their effect on canopy spray deposition, without considering the not negligible ground losses for the UAV-spray application. It should be noted that in our results, the interaction between UAV flight modes and nozzle types had a significant effect on the ground losses (Table 4). When the AI nozzles were adopted, the ground losses decreased in the 1-way band flight, compared to the other flight modes. The lowest ground losses for the conventional nozzles were obtained in the 1-way band flight mode, further confirming that the strategy
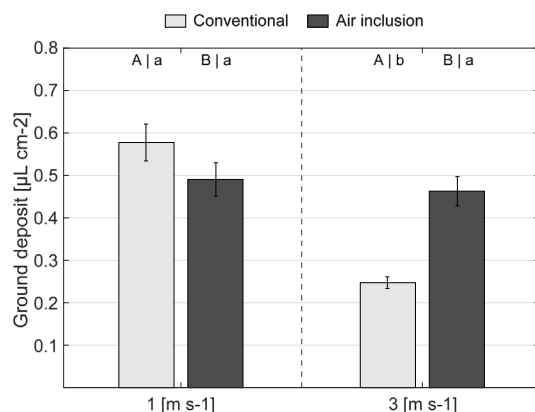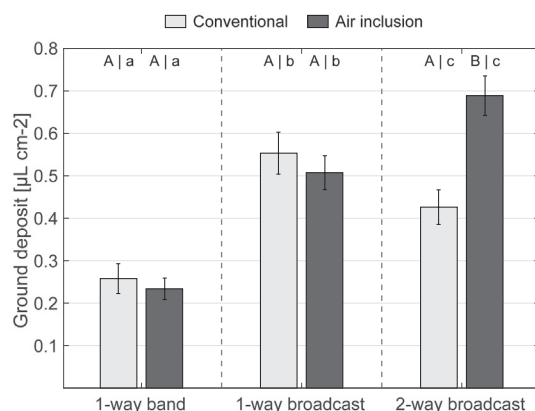
Fig. 8. Average in-field ground losses deposit values [μL cm^{-2}] for different nozzle types (conventional and air inclusion) and UAV cruise speeds (1 and 3 m s^{-1}). Different uppercase letters indicate significant differences between nozzle types per UAV cruise speed whereas lowercase letters indicate significant differences between UAV cruise speeds per nozzle type. The differences are defined according to Tukey's post hoc tests with Bonferroni-adjusted *p*-values ($p < 0.05$). The error bars represent the standard error of the means.

of flying above the vine row, which targets the sprayed liquid on the canopy in trellised vineyards, can be a reliable way to both maximise the efficacy of treatment and minimise ground losses.

Therefore, our results depend on the combination of two factors. First, a technical factor that affects the ground losses according to the configuration of the UAV-spray system (e.g., nozzle type, cruise speed, etc.). Second, the vines canopy area (aerial view) is very small if compared to the inter-row area not covered by the vine rows. Therefore, when the broadcast spray applications were carried out flying perpendicular to the orientation of the rows (Fig. 3), the probability of losing liquid in the inter-row was higher than the probability of hitting the target, and this was demonstrated and represented in Fig. 9.

The strong effects of the UAV flight mode on the ground losses were displayed in Fig. 10, where its significant interaction with the UAV cruise speed (Table 4) is represented. In this case, irrespective of the nozzle types, significantly lower ground spray losses were found when using the 1-way band flight mode at both cruise speeds, namely 1 and 3 m s^{-1}. Also, no differences between the two tested broadcast flight modes were found at the two cruise speeds. On the contrary, the UAV cruise speed deeply affected the ground deposit for both the 1-way broadcast and 2-

Fig. 9. Average in-field ground losses deposit values [μL cm^{-2}] for different nozzle types (conventional and air inclusion) and UAV flight modes (1-way band, 1-way and 2-way broadcast). Different uppercase letters indicate significant differences between nozzle types per UAV flight mode, whereas lowercase letters indicate significant differences between UAV flight modes per nozzle type. The differences are defined according to Tukey's post hoc tests with Bonferroni-adjusted p-values ($p < 0.05$). The error bars represent the standard error of the means.
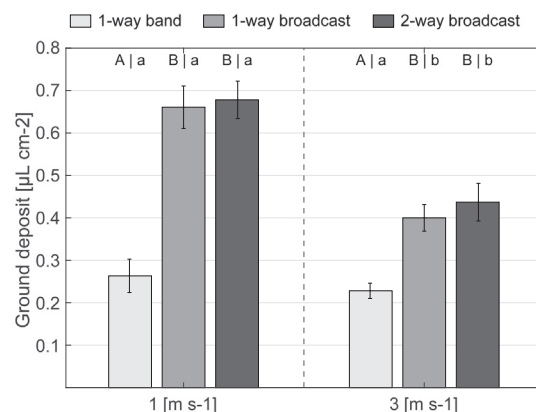
Fig. 10. Average in-field ground losses deposit values [μL cm^{-2}] for different UAV flight modes (1-way band, 1-way and 2-way broadcast) and UAV cruise speeds (1 and 3 m s^{-1}). Different uppercase letters indicate significant differences between UAV flight modes per UAV cruise speed mode, whereas lowercase letters indicate significant differences between UAV cruise speeds per UAV flight mode. The differences are defined according to Tukey's post hoc tests with Bonferroni-adjusted p-values ($p < 0.05$). The error bars represent the standard error of the means.

way broadcast flight modes. Indeed, at the 3 m s^{-1} UAV cruise speed, the ground deposit was reduced by 32 % on average.

The joint analysis of the results obtained for canopy deposition and ground losses allowed the 1-way band flight mode, combined with the UAV cruise speed at 3 m s^{-1}, to be identified as the best parameters to maximise the canopy deposition and at the same time minimise the ground losses, irrespective of the nozzle types used. In any case, the results for the spray coverage in Fig. 7 underline how the very low spray application rate at 3 m s^{-1} is not enough to guarantee an adequate coverage level for efficacious spray application according to the Syngenta evaluation threshold. This suggests that the UAV operational parameters, namely the 1-way band spray application and the 3 m s^{-1} cruise speed, must be combined with a higher spray application rate than those used in our experimental trials (53 L ha^{-1}), possibly by using conventional nozzles characterised by a bigger size.

3.4. In-depth analysis of the 1-way band flight mode

According to the previously discussed results, the statistical analysis was focused on the 1-way band flight mode to investigate the possible effects of the UAV cruise speed and nozzle types on canopy spray deposition in different positions of the canopy, namely the bottom, middle, and top parts (see § 2.3). This latter parameter is critical during aerial spray applications when using UAVs in 3D crops for its effect on canopy spray penetration.

Table 5
Results of the linear mixed model ($p < 0.05$) for the canopy spray deposition [μL cm^{-2}] obtained when testing the 1-way band UAV flight mode.

Model term	DF1	F.ratio	p value [a]
Main effects			
Nozzle type	1	53.551	<0.0001 ***
UAV speed	1	4.111	0.0440 *
Canopy height	2	21.433	<0.0001 ***
Interactions			
Nozzle x Speed	1	7.345	0.0073 **
Nozzle x Height	2	2.108	0.1243 NS
Speed x Height	2	1.158	0.3164 NS
Nozzle x Speed x Height	2	0.174	0.8401 NS

DF2 = 193.
[a] Statistical significance level: NS $p > 0.05$; * $p < 0.05$; ** $p < 0.01$; *** $p < 0.001$.

Furthermore, the effects of the UAV cruise speed and nozzle types on the ground losses for the 1-way band flight mode were further and investigated in-depth.

### 3.4.1. Canopy deposit: spatial canopy spray deposit distribution and canopy penetration

The results of the linear mixed model analysis (Table 5) showed that nozzle type, UAV cruise speed and canopy height had a significant effect on the canopy deposit. The canopy height caused no significant interactions among the tested parameters. Concerning the effects of the nozzle types and the UAV cruise speed, the results reported in Table 5 substantially highlight the main findings already discussed in Figs. 4–6. Indeed, the conventional nozzles used at a UAV cruise speed of 3 m s^{-1} were characterised by a higher canopy spray deposition.

As expected, the canopy height, where the filter papers for the measurements of the canopy spray deposition were placed, significantly affected spray deposition, irrespective of the nozzle types and cruise speeds (Table 5). As shown in Fig. 11, the average canopy deposit at the top of the canopy was about three times higher than the values measured in the middle and at the bottom (grape bunches zone) of the canopy. This result underlines the difficulty for aerial spray applications to penetrate the canopy height from top to bottom. In essence, no matter what the UAV-sprayer configuration was, in all cases the droplets did not easily penetrate the vineyard canopy at full growth stage (1.60 m of vegetative strip height to be penetrated). The difficulties to penetrate the canopy using UAV-spray systems have already been documented by other authors in different 3D crops characterised by different tree shapes such as peach trees (Meng et al., 2018), olive and citrus orchards (Martinez-Guanter et al., 2020), and almond trees (Li et al., 2021). These works showed marked differences in the spray deposition at different canopy heights, and all authors agreed with the great relevance that the downwash airflow field and flight height have on the canopy droplets penetration.

3.4.2. Ground deposit: spatial distribution of the ground losses

Table 6 shows the results obtained from the linear mixed model when testing the effects of the nozzle types, UAV cruise speed, and the distance on the ground from the vineyard rows on the ground losses. The significant interaction between the nozzle types and the UAV cruise speed reflects the results of the linear mixed model presented in Table 4 and already discussed in the previous sections, where the ground losses decrease with the increase of the UAV cruise speed.

Interestingly, the ground losses deposition was significantly affected by the interaction between the distance from the vine row and the UAV cruise
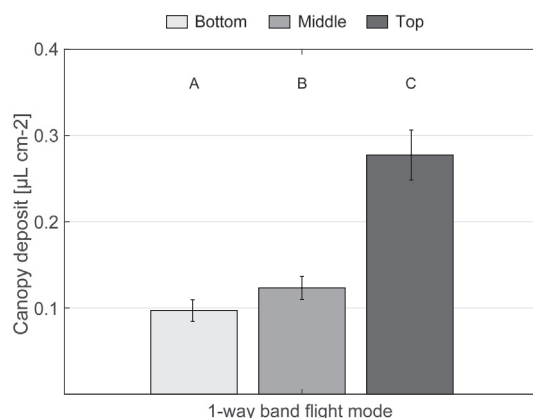
Fig. 11. Average spray canopy deposit values [μL cm^{-2}] for different canopy elevation (bottom, middle and top) in the case of the 1-way band flight mode. Different uppercase letters indicate significant differences between canopy elevations. The differences are defined according to Tukey's post hoc tests with Bonferroni-adjusted p-values ($p < 0.05$). The error bars represent the standard error of the means.

Table 6
Results of the linear mixed model ($p < 0.05$) for the ground losses deposition [μL cm^{-2}] obtained by testing the 1-way band UAV flight mode.

Model term	DF1	F.ratio	p value [a]
Main effects			
Nozzle type	1	0.853	0.3579 NS
UAV speed	1	1.129	0.2904 NS
Distance	2	111.005	<0.0001 ***
Interactions			
Nozzle x Speed	1	5.512	0.0207 *
Nozzle x Distance	2	2.388	0.0967 NS
Speed x Distance	2	17.454	<0.0001 ***
Nozzle x Speed x Distance	2	2.956	0.0564 NS

DF2 = 106.
[a] Statistical significance level: NS $p > 0.05$; * $p < 0.05$; ** $p < 0.01$; *** $p < 0.001$.

speed (Table 6). As expected, the lowest spray losses (Fig. 12) were obtained when the collectors were placed under the vine rows on the ground (0 m from the trunks line, Pos. 1 in Fig. 12) as they were fully covered by the projected canopy area (aerial view), irrespective of the UAV cruise speed. At the lower UAV cruise speed (1 m s^{-1}), the ground deposit detected in the middle of the inter-rows (1.25 m from the row trunks line, both right and left side, Pos. 3 in Fig. 12) was much lower than the one found in the intermediate sampling position (0.625 m from the row trunks line, both right and left side, Pos. 2 in Fig. 12). No differences in the ground deposit between Pos. 2 and 3 were obtained at the 3 m s^{-1} UAV cruise speed. Also, this trend confirms the results reported by Wang et al. (2021) about the downwash airflow field. Indeed, at the 3 m flight height, increasing the UAV cruise speed, the eddies on both sides of the fuselage gradually become larger and gathered towards each other, which will entrain and affect the spatial movement and distribution of the droplets, with a possible lateral movement/expansion of the spray cloud relative to the UAV advancing path.

3.5. Comparison between UAV and airblast sprayers

The results of the comparison between the UAV-spray system application and the conventional airblast sprayer, used as a reference spray application technique, are reported in Fig. 13. For a broad comparison of the two techniques, a low spray application rate (164.6 L ha^{-1}) was applied by
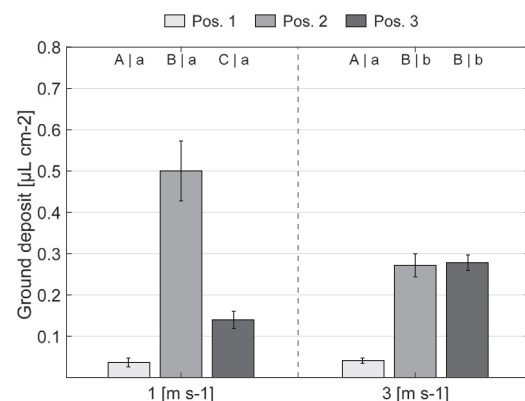
Fig. 12. Average ground losses deposit values [μL cm^{-2}] for different sampling distance positions from the vine row (Pos. 1 = under the canopy, corresponding to the vine trunks line, Pos. 3 = in the middle of the inter row distance, corresponding to 1.25 m from the vine trunks line, and Pos. 2 = between the Pos. 1 and Pos. 3 positions, corresponding to 0.625 m from the vine trunks line) and the UAV cruise speed (1 and 3 m·s^{-1}). Different uppercase letters indicate significant differences between the Petri dishes positions per UAV cruise speed mode, whereas lowercase letters indicate significant differences between the UAV cruise speeds per Petri dishes position. The differences are defined according to Tukey's post hoc tests with Bonferroni-adjusted p-values ($p < 0.05$). The error bars represent the standard error of the means.
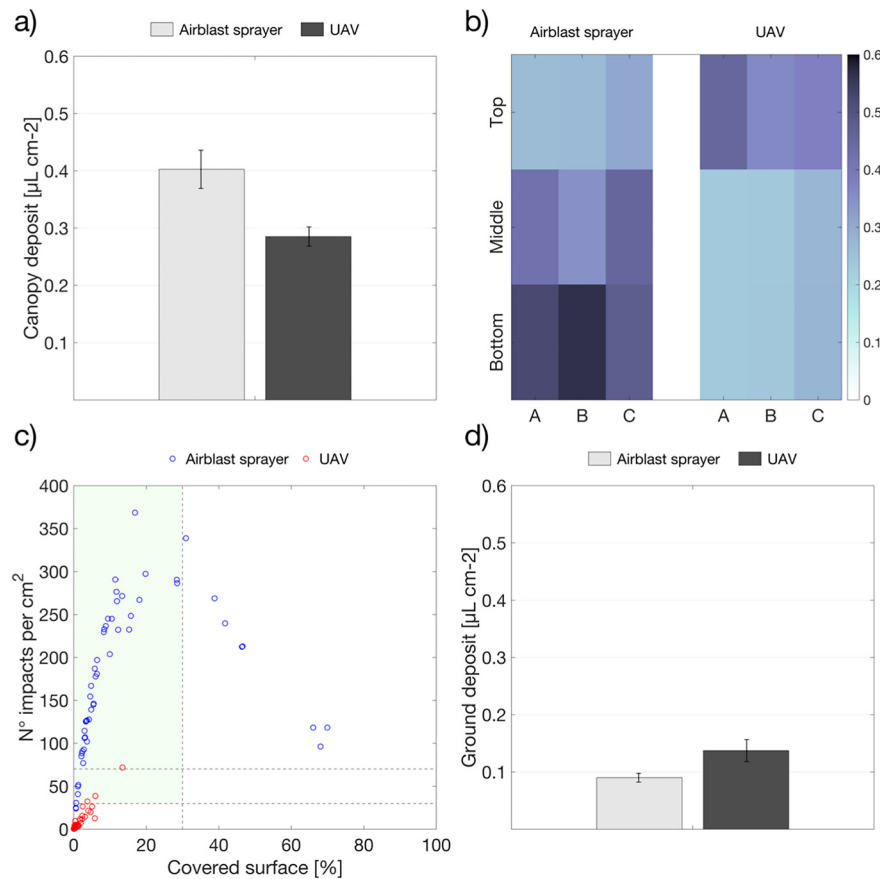
Fig. 13. Comparison between the UAV-spray application technique (1-way band flight mode combined with conventional nozzles at 3 m s^{-1} cruise speed) and the airblast sprayer used as reference. In detail, a) the canopy spray deposition [μL cm^{-2}], b) the spatial distribution of the spray deposit [μL cm^{-2}] within different canopy heights (bottom, middle and top) and depths (A, B and C), c) the relationships between spray coverage (%) and deposit density (n° of stains per cm^2), and d) the ground losses [μL cm^{-2}].

using the airblast sprayer and the standardised deposit values (see § 2.7.1). The airblast sprayer made it possible to obtain a higher canopy spray deposition (Fig. 13a) than the best configuration for the UAV-spray system identified among those tested (Table 1). It can be observed in the colour map of Fig. 13b that the highest spray deposition was obtained in the bottom and top parts of the canopy for the airblast and UAV sprayers, respectively. In essence, the canopy part nearly to the spray and airflow sources was the one characterised by the highest canopy spray deposition. Furthermore, the airblast sprayer achieved, in the top canopy part, values comparable to those measured for the UAV-spray system at the bottom and middle canopy heights. Concerning spray coverage, the airblast sprayer showed the typical trend between surface coverage and deposit density (Grella et al., 2020a and 2022b), with a very high deposit density due to the fine droplet size spectra produced by the Albuz ATR 80 lilac hollow cone nozzles at a 0.5 MPa spray pressure (Table 2). Indeed, only 2 and 6 WSPs were characterised by deposit densities lower than 30 and 70 stains per cm^2 respectively (11 % of the WSPs), while when using the UAV-spray system, the under-sprayed WSPs were 98 % (Fig. 13c). It should be noted that the WSPs data was not standardised to the same spray application rate as it was for the canopy spray deposit.

The ground losses were higher for the UAV-spray system as shown in Fig. 13d, and this was somewhat expected considering that the spray was directed from the UAV-spray system perpendicularly to the ground. The comparison between the two spray application techniques suggests that the UAV-spray system, even in the best adjustment conditions, was characterised by a spray application efficiency that was lower than the one obtained by the airblast sprayer in terms of canopy spray deposition and ground losses. As a final remarks, Fig. 13c further underlines the need to increase the spray application rate when using UAVs in order to

reduce the gap between the airblast and the UAV-spray application techniques in terms of spray coverage. Indeed, with the UAV operated at 3 m s^{-1}, a very low spray application rate equal to 53 L ha^{-1} was applied, thus resulting in a canopy spray deposit density and coverage that are very far from those obtained when using the airblast sprayer operated at low spray application rate (164.6 L ha^{-1}).

4. Conclusions

The experimental field trials allowed the identification of the optimal operational parameters, among those tested, to be used for vineyard spray applications at the full growth stage using a six-rotor UAV equipped with a customised spray application system. From the experimental results it can be concluded that:

i) The parameter that most affected the spray application efficiency was the flight mode. Indeed, the UAV broadcast spray applications in the vineyard at full growth stage were demonstrated not to be feasible as very low canopy spray depositions were measured. Meanwhile, the band spray mode, in which the UAV is aligned with the vine row orientation, made it possible to target the spray on the crop canopy as much as possible, thus maximising the deposition and minimising the off-target losses on the ground. When a band spray application is used, the selection of nozzles characterised by a reduced spray angle is thus of primary importance.

ii) Concurrently, spray application efficiency is deeply affected by the selection of the nozzle type. The air inclusion nozzles, even if representing the best solution for the containment of spray drift, showed a very low amount of canopy spray deposition compared to the conventional

ones. Also, higher canopy ground losses were detected. Therefore, the conventional nozzles proved to be the best solution to significantly increase the canopy deposition and concurrently reduce the in-field off-target losses.

iii) The use of a high UAV cruise speed (3 m s^{-1}) allowed to further increase the canopy spray deposition and reduce spray losses especially when the conventional nozzles were used.

iv) Even if the 1-way band spray application, combined with the conventional nozzles and operated at the 3 m s^{-1} UAV cruise speed, proved to be the best configuration for spray applications in the vineyard at a full growth stage, the very low spray application rate (53 L ha^{-1}) was demonstrated to be insufficient to guarantee an adequate spray deposit density (n° stains per cm^2) for insecticide or fungicide spray applications as under-sprayed WSPs represented >90 % of the total WSPs.

v) The comparison between the best UAV-spray system configuration and the conventional airblast sprayer (operated with a low spray application rate) highlighted the potential for the UAV-spray system to reach spray performances comparable to those obtained by the airblast sprayer. However, the spray application rate must be increased using the UAV-spray system to drastically reduce the under-sprayed situations.

vi) The deposit distribution among different positions in the vine canopy underlines how the relative distance between the spray source and the target is a key parameter irrespective of spray application technique (UAV-spray system vs airblast sprayer).

Based on these results, research is still ongoing and further field trials are planned to define the best spray application rate required in vineyards at different growth stages. Concurrently, new solutions are under evaluation to better target the spray over the canopy, thus increasing the canopy deposition, and, at the same time, reducing the inter-rows ground losses as much as possible. Also, field trials designed to evaluate the biological efficacy of the spray applications when using a UAV-spray system are needed to demonstrate the reliability of such types of spray application techniques in trellised vineyards.

Declaration of competing interest

The authors declare that they have no known competing financial interests or personal relationships that could have appeared to influence the work reported in this paper.

Appendix A

Table A1
Weather conditions recorded during the field trials.

Configuration	Temperature [°C]		RH [%]		Wind speed [m s^{-1}]			Wind direction [azimuth]	
	Mean	Δ h1-h2	Mean	Δ h1-h2	Min	Max	Mean	Dominant	Mean [°]
T1	12.1	−0.36	71.1	0.54	0.45	1.80	1.02	SE	127
T2	20.0	−0.35	30.1	0.22	0.70	2.06	1.17	S	185
T3	21.8	0.05	56.6	0.26	0.05	1.88	0.73	NNW	334
T4	20.9	−0.06	54.1	0.53	0.03	0.70	0.36	NNE	11
T5	20.4	0.04	54.9	0.16	0.08	1.48	0.85	NE	54
T6	21.3	−0.16	23.6	0.47	1.02	1.91	1.53	ESE	111
T7	15.9	−0.28	49.7	0.18	0.51	2.36	1.32	S	172
T8	19.4	0.04	67.1	0.40	0.09	1.89	0.95	NNW	340
T9	21.6	0.59	60.9	−2.53	0.24	1.22	0.56	NW	297
T10	23.5	0.07	53.1	0.11	0.37	0.94	0.71	ENE	83
T11	21.2	−0.03	23.9	0.03	0.59	2.22	1.36	ESE	100
T12	25.0	−0.04	48.8	0.38	0.36	1.64	0.95	S	165
T13	19.7	0.16	28.5	−0.71	0.28	1.13	0.64	N	1

References

Ahmad, F., Qiu, B., Dong, X., Ma, J., Huang, X., Ahmed, S., Chandio, F.A., 2020. Effect of operational parameters of UAV sprayer on spray deposition pattern in target and off-target zones during outer field weed control application. Comput. Electron. Agric. 172, 105350. https://doi.org/10.1016/j.compag.2020.105350.

Aru, F., Gertsis, A., Vellidis, G., Morari, F., 2019. Investigation of spraying efficiency of an aerial spraying system in a super-high density olive grove in Greece. Precision Agriculture '19, pp. 357–363 https://doi.org/10.3920/978-90-8686-888-9_44.

Arvidsson, T., Bergström, L., Kreuger, J., 2011. Spray drift as influenced by meteorological and technical factors. Pest Manag. Sci. 67, 586–598. https://doi.org/10.1002/ps.2114.

ASABE, 2009. ASABE S572.1, Spray Nozzle Classification by Droplet Spectra. American Society of Agricultural Engineers, St. Joseph, MI, p. 4.

Baetens, K., Ho, Q.T., Nuyttens, D., de Schampheleire, M., Endalew, A., Hertog, M., Nicolai, B., Ramon, H., Verboven, P., 2008. Development of a 2-D-diffusion advection model for fast prediction of field drift. Atmos. Environ. 43, 1674–1682. https://doi.org/10.1016/j.atmosenv.2008.12.047.

Barua, D.K., 2005. Beaufort wind scale. In: Schwartz, M.L. (Ed.), Encyclopedia of Coastal Science. Encyclopedia of Earth Science Series. Springer, Dordrecht https://doi.org/10.1007/1-4020-3880-1_45.

Bloise, N., Carreño Ruiz, M., D'Ambrosio, D., Guglieri, G., 2021. Wind tunnel testing of remotely piloted aircraft systems for precision crop-spraying applications. IEEE International Workshop on Metrology for Agriculture and Forestry. 378–383. https://doi.org/10.1109/MetroAgriFor52389.2021.9628600.

Braekman, P., Foque, D., Messens, W., Van Labeke, M.-C., Pieters, J.G., Nuyttens, D., 2010. Effect of spray application technique on spray deposition in greenhouse strawberries and tomatoes. Pest Manag. Sci. 66, 203–212. https://doi.org/10.1002/ps.1858.

Campos, J., Llop, J., Gallart, M., García-Ruiz, F., Gras, A., Salcedo, R., Gil, E., 2019. Development of canopy vigour maps using UAV for site-specific management during vineyard spraying process. Precis. Agric. 20, 1136–1156. https://doi.org/10.1007/s11119-019-09643-z.

Cerruto, E., Manetto, G., Longo, D., Failla, S., Papa, R., 2019. A model to estimate the spray deposit by simulated water sensitive papers. Crop Prot. 124, 104861. https://doi.org/10.1016/j.cropro.2019.104861.

Chen, Y., Ozkan, H.E., Zhu, H., Derksen, R.C., Krause, C.R., 2013. Spray deposition inside tree canopies from a newly developed variable-rate air-assisted sprayer. Trans. ASABE 56, 1263–1272. https://doi.org/10.13031/trans.56.9839.

Chen, H., Lan, Y., Fritz, B.K., Clint Hoffmann, W., Liu, S., 2021. Review of agricultural spraying technologies for plant protection using unmanned aerial vehicle (UAV). Int. J. Agric. Biol. Eng. 14, 38–49. https://doi.org/10.25165/j.ijabe.20211401.5714.

Dekeyser, D., Duga, A.T., Verboven, P., Melese Endalew, A., Hendrickx, N., Nuyttens, D., 2013. Assessment of orchard sprayers using laboratory experiments and computational fluid dynamics modelling. Biosyst. Eng. 114, 157–169. https://doi.org/10.1016/j.biosystemseng.2012.11.013.

EC, 2019. Communication from the Commission to the European Parliament, the European Council, the Council, the European Economic and Social Committee and the Committee of the Regions. The European Green Deal COM/2019/640 final. https://eur-lex.europa.eu/legal-content/EN/TXT/?uri=COM%3A2019%3A640%3AFIN.

EC, Commission Regulation No 128/2009 of 13 February 2009 establishing the standard import values for determining the entry price of certain fruit and vegetables https://eur-lex.europa.eu/eli/reg/2009/128/oj.

EFSA (European Food Safety Authority), Carrasco Cabrera, L., Medina Pastor, P., 2021. The 2019 European Union report on pesticide residues in food. EFSA J. 19, e06491. https://doi.org/10.2903/j.efsa.2021.6491.

Fabiani, S., Vanino, S., Napoli, R., Zajíček, A., Duffková, R., Evangelou, E., Nino, P., 2020. Assessment of the economic and environmental sustainability of variable rate technology (VRT) application in different wheat intensive European agricultural areas. A water energy food nexus approach. Environ. Sci. Policy 114, 366–376. https://doi.org/10.1016/j.envsci.2020.08.019.

Fox, R.D., Derksen, R.C., Cooper, J.A., Krause, C.R., Ozkan, H.E., 2003. Visual image system measurements of spray deposits using water-sensitive paper. Appl. Eng. Agric. 19, 549–552. https://doi.org/10.13031/2013.15315.

Garcerá, C., Moltó, E., Chueca, P., 2011. Effect of spray volume of two organophosphate pesticides on coverage and on mortality of California red scale Aonidiella aurantii (Maskell). Crop Prot. 30, 693–697. https://doi.org/10.1016/j.cropro.2011.02.019.

Gil, E., Escolà, A., 2009. Design of a decision support method to determine volume rate for vineyard spraying. Appl. Eng. Agric. 25, 145–151.

Gil, E., Gallart, M., Balsari, P., Marucco, P., Almajano, M.P., Llop, J., 2015. Influence of wind velocity and wind direction on measurements of spray drift potential of boom sprayers using drift test bench. Agric. For. Meteorol. 202, 94–101. https://doi.org/10.1016/j.agrformet.2014.12.002.

Giles, D.K., Billing, R., 2015. Deployment and performance of a UAV for crop spraying. Chem. Eng. Trans. 44, 307–312. https://doi.org/10.3303/CET1544052.

Grella, M., Gallart, M., Marucco, P., Balsari, P., Gil, E., 2017. Ground deposition and airborne spray drift assessment in vineyard and orchard: the influence of environmental variables and sprayer settings. Sustainability 9, 728. https://doi.org/10.3390/su9050728.

Grella, M., Marucco, P., Balsari, P., 2019. Toward a new method to classify the airblast sprayers according to their potential drift reduction: comparison of direct and new indirect measurement methods. Pest Manag. Sci. 75, 2219–2235. https://doi.org/10.1002/ps.5354.

Grella, M., Miranda-Fuentes, A., Marucco, P., Balsari, P., 2020a. Field assessment of a newly-designed pneumatic spout to contain spray drift in vineyards: evaluation of canopy distribution and off-target losses. Pest Manag. Sci. 76, 4173–4191. https://doi.org/10.1002/ps.5975.

Grella, M., Miranda-Fuentes, A., Marucco, P., Balsari, P., Gioelli, F., 2020b. Development of drift-reducing spouts for vineyard pneumatic sprayers: measurement of droplet size spectra generated and their classification. Appl. Sci. 10, 7826. https://doi.org/10.3390/app10217826.

Grella, M., Marucco, P., Zwertvaegher, I., Gioelli, F., Bozzer, C., Biglia, A., et al., 2022a. The effect of fan setting, air-conveyor orientation and nozzle configuration on airblast sprayer efficiency: insights relevant to trellised vineyards. Crop Prot. 155, 105921. https://doi.org/10.1016/j.cropro.2022.105921.

Grella, M., Gioelli, F., Marucco, P., Zwertvaegher, I., Mozzanini, E., Mylonas, N., Balsari, P., 2022b. Field assessment of a pulse width modulation (PWM) spray system applying different spray volumes: duty cycle and forward speed effects on vines spray coverage. Precis. Agric. 23, 219–252. https://doi.org/10.1007/s11119-021-09835-6.

Guo, S., Li, J., Yao, W., Zhan, Y., Li, Y., Shi, Y., 2019. Distribution characteristics on droplet deposition of wind field vortex formed by multi-rotor UAV. PLoS One 14, e0220024. https://doi.org/10.1371/journal.pone.0220024.

He, X., Bonds, J., Herbst, A., Langenakens, A., 2017. Recent development of unmanned aerial vehicle for plant protection in East Asia. Int. J. Agric. Biol. Eng. 10, 18–30. https://doi.org/10.3965/j.ijabe.20171003.3248.

Herbst, A., Bonds, J., Wang, Z., Zeng, A., He, X., Goff, P., 2020. The influence of Unmanned Agricultural Aircraft System design on spray drift. J. Kult. 72, 1–11. https://doi.org/10.5073/JfK.2020.01.01.

Hołownicki, R., Doruchowski, G., Świechowski, W., Jaeken, P., 2002. Methods of evaluation of spray deposit and coverage on artificial targets. Electron. J. Pol. Agric. Univ. 5.

Huang, H., Deng, J., Lan, Y., Yang, A., Deng, X., Zhang, L., 2018. A fully convolutional network for weed mapping of unmanned aerial vehicle (UAV) imagery. PLoS One 13, e0196302. https://doi.org/10.1371/journal.pone.0196302.

Hunter, J.E., Gannon, T.W., Richardson, R.J., Yelverton, F.H., Leon, R.G., 2020. Integration of remote-weed mapping and an autonomous spraying unmanned aerial vehicle for site-specific weed management. Pest Manag. Sci. 76, 1386–1392. https://doi.org/10.1002/ps.5651.

Imperatore, G., Ghirardelli, A., Strinna, L., Baldoin, C., Pozzebon, A., Zanin, G., et al., 2021. Evaluation of a fixed spraying system for phytosanitary treatments in heroic viticulture in north-eastern Italy. Agriculture 11, 833. https://doi.org/10.3390/agriculture11090833.

International Organization for Standardization (ISO), 2018. ISO 10625:2018: Equipment for Crop Protection — Sprayer Nozzles — Colour Coding for Identification. International Organization for Standardization, Geneva, Switzerland, pp. 1–5.

Intrieri, C., Poni, S., 1995. Integrated evolution of trellis training systems and machines to improve grape quality and vintage quality of mechanized Italian vineyards. Am. J. Enol. Vitic. 46, 116–127.

Jensen, P.K., Olesen, M.H., 2014. Spray mass balance in pesticide application: a review. Crop Prot. 61, 23–31. https://doi.org/10.1016/j.cropro.2014.03.006.

Kamilaris, A., Kartakoullis, A., Prenafeta-Boldú, F.X., 2017. A review on the practice of big data analysis in agriculture. Comput. Electron. Agric. 143, 23–37. https://doi.org/10.1016/j.compag.2017.09.037.

Kasner, E.J., Prado, J.B., Yost, M.G., Fenske, R.A., 2021. Examining the role of wind in human illness due to pesticide drift in Washington state, 2000–2015. Environ. Health 20, 26. https://doi.org/10.1186/s12940-021-00693-3.

Kayad, A., Sozzi, M., Gatto, S., Whelan, B., Sartori, L., Marinello, F., 2021. Ten years of corn yield dynamics at field scale under digital agriculture solutions: a case study from North Italy. Comput. Electron. Agric. 185, 106126. https://doi.org/10.1016/j.compag.2021.106126.

Kellogg, R.L., Nehring, R.F., Grube, A., Goss, D.W., Plotkin, S., 2002. Environmental indicators of pesticide leaching and runoff from farm fields. Agric.Prod. 2, 213–256. https://doi.org/10.1007/978-1-4615-0851-9_9.

Kharim, M.N., Wayayok, A., Shariff, A.R.M., Abdullah, A.F., Husin, E.M., 2019. Droplet deposition density of organic liquid fertilizer at low altitude UAV aerial spraying in rice cultivation. Comput. Electron. Agric. 167, 105045. https://doi.org/10.1016/j.compag.2019.105045.

Li, L., Liu, Y., He, X., Song, J., Zeng, A., Zhichong, W., Tian, L., 2018. Assessment of spray deposition and losses in the apple orchard from agricultural unmanned aerial vehicle in China. 2018 ASABE Annual International Meeting https://doi.org/10.13031/aim.201800504.

Li, X., Giles, D.K., Niederholzer, F.J., Andaloro, J.T., Lang, E.B., Watson, L.J., 2021. Evaluation of an unmanned aerial vehicle as a new method of pesticide application for almond crop protection. Pest Manag. Sci. 77, 527–537. https://doi.org/10.1002/ps.6052.

Lian, Q., Tan, F., Fu, X., Zhang, P., Liu, X., Zhang, W., 2019. Design of precision variable-rate spray system for unmanned aerial vehicle using automatic control method. Int. J. Agric. Biol. Eng. 12, 29–35. https://doi.org/10.25165/j.ijabe.20191202.4701.

Liu, Y., Li, L., Liu, Y., He, X., Song, J., Zeng, A., et al., 2020. Assessment of spray deposition and losses in an apple orchard with an unmanned agricultural aircraft sSystem in China. Trans. ASABE 63, 619–627. https://doi.org/10.13031/trans.13233.

Llorens, J., Gil, E., Llop, J., Escolà, A., 2010. Variable rate dosing in precision viticulture: use of electronic devices to improve application efficiency. Crop Prot. 29, 239–248. https://doi.org/10.1016/j.cropro.2009.12.022.

Lorenz, D.H., Eeichhorn, K.W., Bleiholder, H., Klose, R., Meier, U., Weber, E., 1995. Growth stages of the grapevine: phenological growth stages of the grapevine (Vitis vinifera L. ssp. vinifera)—codes and descriptions according to the extended BBCH scale. Aust. J. Grape Wine Res. 1, 100–103. https://doi.org/10.1111/j.1755-0238.1995.tb00085.x.

Lou, Z., Xin, F., Han, X., Lan, Y., Duan, T., Fu, W., 2018. Effect of unmanned aerial vehicle flight height on droplet distribution, drift and control of cotton aphids and spider mites. Agronomy 8, 187. https://doi.org/10.3390/agronomy8090187.

Mammarella, M., Comba, L., Biglia, A., Dabbene, F., Gay, P., 2020. Cooperative agricultural operations of aerial and ground unmanned vehicles. IEEE International Workshop on Metrology for Agriculture And Forestry. 224–229. https://doi.org/10.1109/MetroAgriFor50201.2020.9277573.

Mammarella, M., Comba, L., Biglia, A., Dabbene, F., Gay, P., 2021a. Cooperation of unmanned systems for agricultural applications: a theoretical framework. Biosyst. Eng. https://doi.org/10.1016/j.biosystemseng.2021.11.008 In Press.

Mammarella, M., Comba, L., Biglia, A., Dabbene, F., Gay, P., 2021b. Cooperation of unmanned systems for agricultural applications: a case study in a vineyard. Biosyst. Eng. https://doi.org/10.1016/j.biosystemseng.2021.12.010 In Press.

Martinez-Guanter, J., Agüera, P., Agüera, J., Pérez-Ruiz, M., 2020. Spray and economics assessment of a UAV-based ultra-low-volume application in olive and citrus orchards. Precis. Agric. 21, 226–243. https://doi.org/10.1007/s11119-019-09665-7.

Marucco, P., Balsari, P., Grella, M., Pugliese, M., Eberle, D., Gil Moya, E., et al., 2019. OPTIMA EU project: Main goal and first results of inventory of current spray practices in vineyards and orchards. Proceedings of SUPROFRUIT 2019, 15th Workshop on Spray Application And Precision Technology in Fruit Growing, pp. 99–100 http://www.emr.ac.uk/wp-content/uploads/2019/07/15thSpraWkshpInsppPDF.pdf.

Meng, Y., Lan, Y., Mei, G., Guo, Y., Song, J., Wang, Z., 2018. Effect of aerial spray adjuvant applying on the efficiency of small unmanned aerial vehicle for wheat aphids control. Int. J. Agric. Biol. Eng. 11, 46–53. https://doi.org/10.25165/j.ijabe.20181105.4298.

Meng, Y., Su, J., Song, J., Chen, W.-H., Lan, Y., 2020. Experimental evaluation of UAV spraying for peach trees of different shapes: effects of operational parameters on droplet distribution. Comput. Electron. Agric. 170, 105282. https://doi.org/10.1016/j.compag.2020.105282.

Miranda-Fuentes, A., Rodríguez-Lizana, A., Gil, E., Agüera-Vega, J., Gil-Ribes, J.A., 2015. Influence of liquid-volume and airflow rates on spray application quality and homogeneity in super-intensive olive tree canopies. Sci. Total Environ. 537, 250–259. https://doi.org/10.1016/j.scitotenv.2015.08.012.

Miranda-Fuentes, A., Llorens, J., Rodríguez-Lizana, A., Cuenca, A., Gil, E., Blanco-Roldán, G.L., Gil-Ribes, J.A., 2016. Assessing the optimal liquid volume to be sprayed on isolated olive trees according to their canopy volumes. Sci. Total Environ. 568, 296–305. https://doi.org/10.1016/j.scitotenv.2016.06.013.

Nuyttens, D., Windey, S., Sonck, B., 2004. Optimisation of a vertical spray boom for greenhouse spray applications. Biosyst. Eng. 89, 417–423. https://doi.org/10.1016/j.biosystemseng.2004.08.016.

Nuyttens, D., Baetens, K., de Schampheleire, M., Sonck, B., 2007. Effect of nozzle type, size and pressure on spray droplet characteristics. Biosyst. Eng. 97, 333–345. https://doi.org/10.1016/j.biosystemseng.2007.03.001.

O'Shaughnessy, S.A., Evett, S.R., Colaizzi, P.D., 2015. Dynamic prescription maps for site-specific variable rate irrigation of cotton. Agric. Water Manag. 159, 123–138. https://doi.org/10.1016/j.agwat.2015.06.001.

OECD, Report on the State of the Knowledge – Literature Review on Unmanned Aerial Spray Systems in Agriculture series on Pesticides, 2021. No.105. https://www.oecd.org/chemicalsafety/pesticides-biocides/literature-review-on-unmanned-aerial-spray-systems-in-agriculture.pdf. (Accessed 3 November 2022).

Palleja, T., Landers, A.J., 2017. Real time canopy density validation using ultrasonic envelope signals and point quadrat analysis. Comput. Electron. Agric. 134, 43–50. https://doi.org/10.1016/j.compag.2017.01.012.

Perez-Ruiz, M., Martínez-Guanter, J., Upadhyaya, S.K., 2021. Chapter 15 - high-precision GNSS for agricultural operations. GPS And GNSS Technology in Geosciences, pp. 299–335 https://doi.org/10.1016/B978-0-12-818617-6.00017-2.

Pergher, G., Petris, R., 2008. The effect of air flow rate on spray deposition in a guyot-trained vineyard.

Pinheiro, J., Bates, D., DebRoy, S., Sarkar, D., R Core Team, 2021. _nlme: Linear and Nonlinear Mixed Effects Models_. R package version 3.1-153. https://CRAN.R-project.org/package=nlme.

Popp, J., Pető, K., Nagy, J., 2013. Pesticide productivity and food security.A review. Agron. Sustain. Dev. 33, 243–255. https://doi.org/10.1007/s13593-012-0105-x.

Qin, W.-C., Qiu, B.-J., Xue, X.-Y., Chen, C., Xu, Z.-F., Zhou, Q.-Q., 2016. Droplet deposition and control effect of insecticides sprayed with an unmanned aerial vehicle against plant hoppers. Crop Prot. 85, 79–88. https://doi.org/10.1016/j.cropro.2016.03.018.

Qin, W., Xue, X., Zhang, S., Gu, W., Wang, B., 2018. Droplet deposition and efficiency of fungicides sprayed with small UAV against wheat powdery mildew. Int. J. Agric. Biol. Eng. 11, 27–32. https://doi.org/10.25165/j.ijabe.20181102.3157.

R Core Team, 2021. R: A Language And Environment for Statistical Computing. R Foundation for Statistical Computing, Vienna, Austria https://www.R-project.org/.

Radoglou-Grammatikis, P., Sarigiannidis, P., Lagkas, T., Moscholios, I., 2020. A compilation of UAV applications for precision agriculture. Comput. Netw. 172, 107148. https://doi.org/10.1016/j.comnet.2020.107148.

Raikwar, S., Wani, L.J., Arun Kumar, S., Sreenivasulu Rao, M., 2018. Hardware-in-the-loop test automation of embedded systems for agricultural tractors. Measurement 133, 271–280. https://doi.org/10.1016/j.measurement.2018.10.014.

Rani, L., Thapa, K., Kanojia, N., Sharma, N., Singh, S., Singh Grewal, A., et al., 2021. An extensive review on the consequences of chemical pesticides on human health and environment. J. Clean. Prod. 283, 124657. https://doi.org/10.1016/j.jclepro.2020.124657.

Rincón, V.J., Grella, M., Marucco, P., Eloi Alcatrão, L., Sanchez-Hermosilla, J., Balsari, P., 2020. Spray performance assessment of a remote-controlled vehicle prototype for pesticide application in greenhouse tomato crops. Sci. Total Environ. 726, 138509. https://doi.org/10.1016/j.scitotenv.2020.138509.

Russell, V.L., 2021. emmeans: Estimated Marginal Means, aka Least-Squares Means. R package version 1.7.0. https://CRAN.R-project.org/package=emmeans.

Sabzevari, S., Hofman, J., 2022. A worldwide review of currently used pesticides' monitoring in agricultural soils. Sci. Total Environ. 812, 152344. https://doi.org/10.1016/j.scitotenv.2021.152344.

Salcedo, R., Zhu, H., Zhang, Z., Wei, Z., Chen, L., Ozkan, E., et al., 2020. Foliar deposition and coverage on young apple trees with PWM-controlled spray systems. Comput. Electron. Agric. 178, 105794. https://doi.org/10.1016/j.compag.2020.105794.

Salcedo, R., Zhu, H., Ozkan, E., Falchieri, D., Zhang, Z., Wei, Z., 2021. Reducing ground and airborne drift losses in young apple orchards with PWM-controlled spray systems. Comput. Electron. Agric. 189, 106389. https://doi.org/10.1016/j.compag.2021.106389.

Salyani, M., Zhu, H., Sweeb, R.D., Pai, N., 2013. Assessment of spray distribution with water-sensitive paper. Agric. Eng. Int.CIGR J. 15, 101–111.

Sarri, D., Martelloni, L., Rimediotti, M., Lisci, R., Lombardo, S., Vieri, M., 2019. Testing a multi-rotor unmanned aerial vehicle for spray application in high slope terraced vineyard. J. Agric. Eng. 50, 38–47. https://doi.org/10.4081/jae.2019.853.

Sassu, A., Gambella, F., Ghiani, L., Mercenaro, L., Caria, M., Pazzona, A.L., 2021. Advances in unmanned aerial system remote sensing for precision viticulture. Sensors 21, 956. https://doi.org/10.3390/s21030956.

Schriever, C.A., von der Ohe, P.C., Liess, M., 2007. Estimating pesticide runoff in small streams. Chemosphere 68, 2161–2171. https://doi.org/10.1016/j.chemosphere.2007.01.086.

Sinha, R., Ranjan, R., Khot, L.R., Hoheisel, G.-A., Grieshop, M.J., 2020. Comparison of within canopy deposition for a solid set canopy delivery system (SSCDS) and an axial–fan airblast sprayer in a vineyard. Crop Prot. 132, 105124. https://doi.org/10.1016/j.cropro.2020.105124.

Tang, Y., Hou, C.J., Luo, S.M., Lin, J.T., Yang, Z., Huang, W.F., 2018. Effects of operation height and tree shape on droplet deposition in citrus trees using an unmanned aerial vehicle. Comput. Electron. Agric. 148, 1–7. https://doi.org/10.1016/j.compag.2018.02.026.

TOPPS-Prowadis Project, 2014. Best management practices to reduce spray drift. Available at http://www.topps-life.org/.

Vitali, M., Tamagnone, M., La Iacona, T., Lovisolo, C., 2013. Measurement of grapevine canopy leaf area by using an ultrasonic-based method. OENO One 47, 183–189. https://doi.org/10.20870/oeno-one.2013.47.3.1551.

Vymazal, J., Březinová, T., 2015. The use of constructed wetlands for removal of pesticides from agricultural runoff and drainage: a review. Environ. Int. 75, 11–20. https://doi.org/10.1016/j.envint.2014.10.026.

Wang, S., Song, J., He, X., Song, L., Wang, X., Wang, C., et al., 2017. Performances evaluation of four typical unmanned aerial vehicles used for pesticide application in China. Int. J. Agric. Biol. Eng. 10, 22–31. https://doi.org/10.25165/j.ijabe.20171004.3219.

Wang, J., Lan, Y., Zhang, H., Zhang, Y., Wen, S., Yao, W., et al., 2018. Drift and deposition of pesticide applied by UAV on pineapple plants under different meteorological conditions. Int. J. Agric. Biol. Eng. 11, 5–12. https://doi.org/10.25165/j.ijabe.20181106.4038.

Wang, G., Lan, Y., Qi, H., Chen, P., Hewitt, A., Han, Y., 2019a. Field evaluation of an unmanned aerial vehicle (UAV) sprayer, effect of spray volume on deposition and the control of pests and disease in wheat. Pest Manag. Sci. 75, 1546–1555. https://doi.org/10.1002/ps.5321.

Wang, G., Lan, Y., Yuan, H., Qi, H., Chen, P., Ouyang, F., Han, Y., 2019b. Comparison of spray deposition, control efficacy on wheat aphids and working efficiency in the wheat field of the unmanned aerial vehicle with boom sprayer and two conventional knapsack sprayers. Appl. Sci. 9, 218. https://doi.org/10.3390/app9020218.

Wang, J., Lan, Y., Yao, W., Chen, P., Wang, G., Chen, S., 2020. Aerial spraying application of multi-rotor unmanned aerial vehicle on areca trees. Int. J. Precis. Agric. Aviat. 3, 51–64. https://doi.org/10.33440/j.ijpaa.20200304.134.

Wang, C., Herbst, A., Zeng, A., Wongsuk, S., Qiao, B., Qi, P., et al., 2021. Assessment of spray deposition, drift and mass balance from unmanned aerial vehicle sprayer using an artificial vineyard. Sci. Total Environ. 777, 146181. https://doi.org/10.1016/j.scitotenv.2021.146181.

Wen, S., Han, J., Ning, Z., Lan, Y., Yin, X., Zhang, J., et al., 2019. Numerical analysis and validation of spray distributions disturbed by quad- T rotor drone wake at different flight speeds. Comput. Electron. Agric. 166, 105036. https://doi.org/10.1016/j.compag.2019.105036.

Wilson, J.W., 1963. Estimation of foliage denseness and foliage angle by inclined point quadrats. Aust. J. Bot. 11, 95–105. https://doi.org/10.1071/BT9630095.

Xu, M., Liu, M., Liu, F., Zheng, N., Tang, S., Zhou, J., et al., 2021. A safe, high fertilizer-efficiency and economical approach based on a low-volume spraying UAV loaded with chelated-zinc fertilizer to produce zinc-biofortified rice grains. J. Clean. Prod. 323, 129188. https://doi.org/10.1016/j.jclepro.2021.129188.

Xue, X., Lan, Y., Sun, Z., Chang, C., Hoffmann, W.C., 2016. Develop an unmanned aerial vehicle based automatic aerial spraying system. Comput. Electron. Agric. 128, 58–66. https://doi.org/10.1016/j.compag.2016.07.022.

Zhan, Y., Chen, P., Xu, W., Chen, S., Han, Y., Lan, Y., et al., 2022. Influence of the downwash airflow distribution characteristics of a plant protection UAV on spray deposit distribution. Biosyst. Eng. 216, 32–45. https://doi.org/10.1016/j.biosystemseng.2022.01.016.

Zhang, P., Deng, L., Lyu, Q., He, S.L., Yi, S.L., Liu, Y.D., et al., 2016. Effects of citrus tree-shape and spraying height of small unmanned aerial vehicle on droplet distribution. Int. J. Agric. Biol. Eng. 9, 45–52. https://doi.org/10.3965/j.ijabe.20160904.2178.

Zhang, X.-Q., Song, X.-P., Liang, Y.-J., Qin, Z.-Q., Zhang, B.-Q., Wei, J.-J., Wu, J.-M., 2020. Effects of spray parameters of drone on the droplet deposition in sugarcane canopy. Sugar Tech 22, 583–588. https://doi.org/10.1007/s12355-019-00792-z.

Zhu, H., Salyani, M., Fox, R.D., 2011. A portable scanning system for evaluation of spray deposit distribution. Comput. Electron. Agric. 76, 38–43. https://doi.org/10.1016/j.compag.2011.01.003.